Primary Oxide Latent Storage and Spillover Enabling Electrocatalysts with Reversible Oxygen Electrode Properties and the Alterpolar Revertible (PEMFC versus WE) Cell

ARTICLE *in* THE JOURNAL OF PHYSICAL CHEMISTRY C · MARCH 2014

Impact Factor: 4.77 · DOI: 10.1021/jp412292w

THE JOURNAL OF PHYSICAL CHEMISTRY C

Feature Article

pubs.acs.org/JPCC

Primary Oxide Latent Storage and Spillover Enabling Electrocatalysts with Reversible Oxygen Electrode Properties and the Alterpolar Revertible (PEMFC versus WE) Cell

Milan M. Jaksic,[†,‡] Gianluigi A. Botton,[§] Georgios D. Papakonstantinou,[†] Feihong Nan,[§] and Jelena M. Jaksic*[,†]

[†]Institute of Chemical Engineering Sciences, FORTH, GR-26504 Patras, Greece

[‡]Faculty of Agriculture, University of Belgrade, 11030 Belgrade, Serbia

[§]Department of Materials Science & Engineering, McMaster University, 1280 Main Street West, Hamilton, Ontario, L8S 4M1, Canada

ABSTRACT: Surface *in* and *ex situ* analysis have shown that in the course of cathodic oxygen reduction (ORR), all along the reversible potential range (the low slope Tafel plots, about 30 mVs/dec), nanostructured Pt electrocatalyst is covered by the interfering primary (Pt−OH) and surface (Pt═O) oxide mixture, while the higher polarization (120 mVs/dec) characterizes electrocatalytic surface deprived from these oxides and, consequently, the reaction mechanism of direct electron exchange on clean electrode surface. The substantial difference between the standard RHE (reversible hydrogen electrode) and ROE (reversible oxygen electrode), is that the former implies spontaneous hydrogen adsorption, fast H-adatoms (Pt−H) effusion and reversible electrode behavior ($Pt(H_2)/Pt-H/H_3O^+$), while the latter features the strong irreversible Pt═O adsorptive strength, and which is more significant, missing the Pt−OH spillover within the critical potential range between the primary oxide adsorption/desorption peaks position and oxygen evolving limits in both potentiodynamic scan directions (or the imposed polarization energy barrier of about 600 mVs). Since the Pt−OH presence and spillover are unavoidable decisive and indispensable for establishing the ROE properties, and thermodynamic electrode equilibrium ($Pt(O_2)/Pt-OH/Pt{=}O/OH^-$), within the pronounced high polarization broad potential range, such spillover species has the same meaning and significance for the ROE as Pt−H plays for the RHE. Thence, to fill such a high polarization gap, the guiding concept implies homogeneous nanostructured distribution and selective grafting while interactive hypo-hyper-d-d-interelectronic bonding of Pt nanoclusters upon various mixed valence hypo-d-oxide supports, primarily Nb_2O_5,TiO_2 (or Ta_2O_5,TiO_2), because of their much thermally advanced electronic conductivity and extra high stability. In such a constellation, nanoparticles of Pt and solid oxides establish the so-called SMSIs (strong metal−support interactions), the strongest ones in all of chemistry, together with advanced electron conductive transfer, while the exposed surface of the latter undergoes spontaneous dissociative adsorption of water molecules ($Nb_2O_5 \rightarrow 2\ Nb(OH)_5$), and thereby becomes, along with continuous further water vapor supply, the undisturbed and almost unlimited, (alike electrons in metals) renewable latent storage and spillover source of the Pt−OH all along the potential axis between oxygen and hydrogen evolving limits, with inexhaustible abilities of further optimizations. The reversible alterpolar changes instantaneously result by the spillover of H-adatoms with corresponding bronze type (Pt/H_xNbO_5, $x \approx 0.3$) electrocatalysts under cathodic, and/or its hydrated state ($Pt/Nb(OH)_5$), responsible for Pt−OH effusion, under anodic polarization. This way there establishes the reversibly revertible alterpolar bronze features ($Pt/H_xNbO_5 \leftrightarrow Pt/Nb(OH)_5$), as the thermodynamic equilibrium, and thereby substantially advanced electrocatalytic properties of these composite interactive electrocatalysts for both oxygen and hydrogen electrode reactions, in particular unique and superior for the revertible (proton exchange membrane fuel cell (PEMFC) versus water electrolysis (WE)) cells.

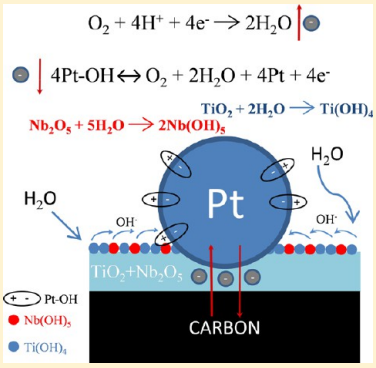

INTRODUCTION

Ever since Sir William Grove invented fuel cells (FCs), electrocatalysts with reversible oxygen electrode (ROE) properties have become the main imperative target and challenge in electrochemistry of aqueous and PEM media, while its substantiation is the subject matter of the present paper.

The substance is that hydrogen molecules undergo spontaneous adsorptive dissociation on plain Pt (Pt/C), and H-adatoms (Pt−H) establish thermodynamic equilibrium of the RHE (reversible hydrogen electrode, ($Pt(H_2)/Pt-H/H_3O^+$)). Which species and from where might they come, or can they be spontaneously stored and enabled to establish and continuously keep the reversible ORR (cathodic oxygen reduction) and/or OER (oxygen evolution reaction) of advanced

Received: December 16, 2013
Revised: February 14, 2014

dx.doi.org/10.1021/jp412292w | J. Phys. Chem. C XXXX, XXX, XXX−XXX

electrocatalytic properties both within the oxygen and hydrogen evolving limits, and the thermodynamic equilibrium of the ROE as the limiting value ($j \rightarrow 0$), and both the reversible hydrogen fueled low and medium temperature proton exchange membrane fuel cells (L&MT PEMFCs) at fixed rate or capacity?

All energy chart diagrams (Figure 1a), so far scanned from LT PEMFCs with nanostructured Pt/C electrocatalysts, like a specific potentiodynamic spectrum, show a sharp potential drop (or polarization) accompanied by negligible current values, initiating almost at the thermodynamic ROE value (1.29 V vs RHE), and extending down to the certain voltage plateau established at about 0.6 V vs RHE, or that the amount of energy is waste for more than half of theoretically available power yields (cf. ref 1). The interconnected cyclic voltammograms (Figure 1b), scanned within the hydrogen and oxygen potential evolving limits, when interrelated with the same corresponding former voltage axis (Figure 1a), in addition, heuristically indicate and straightforwardly reveal that the stable potential range (approximately like a plateau) in the energy conversion coincides with and corresponds to the pronounced substantially reversible adsorption−desorption peak locations of the Pt−OH growth and removal:[2−5]

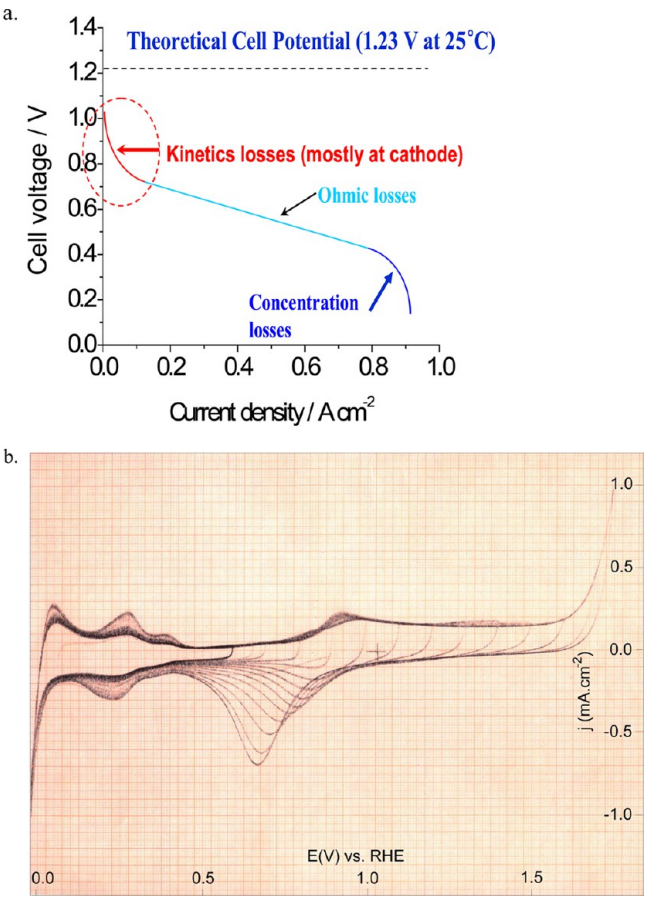

Figure 1. (a) Classical and characteristic energy chart diagram for nanostructured Pt/C electrocatalyst in LT PEMFCs. (b) Cyclic voltammograms of polycrystalline Pt scanned in 0.1 M NaOH at a sweep rate of 100 mV·s^{-1}.

$$Pt + 2H_2O \leftrightarrow Pt{-}OH + H_3O^+ + e^- \quad (1)$$

The latter implies extremely fast reaction occurring in both scan directions, so that the polarization determining species (PDS) along the broader potential range, or the main obstacle slowing down the ORR rate and preventing it from proceeding faster and eventually approach its reversible properties, undoubtedly arises to be the strongly irreversible adsorbed and highly polarizable surface oxide (Pt═O),

$$Pt{-}OH + H_2O \rightarrow Pt{=}O + H_3O^+ + e^- \quad (2)$$

but by no means such an extremely reversible primary oxide (Pt−OH). For such, so far mostly in the wasting energy range, except (partially less) when dealing with some advanced specific electrocatalysts, this is clearly revealed from the polarization shape of potentiodynamic spectra changes within the critical potential interval relative to these typical energy charts both scanned in acidic[6] and alkaline (Figure1b) aqueous media. Meanwhile, the most significant observation and facts are that such typical highly pronounced fast reversible reactions, like eq 1 for the Pt−OH adsorptive and desorptive spillover, always occur *independently* in both directions for themselves, and consequently can hardly be influenced by others, except the typical interfering species, or by some still faster interacting components or accompanying electrode reactions (see, for example, the inferred issue and the effect of anodic formaldehyde oxidation below).

The substantial problem in fact is that the peak values of the fast reversible reaction of the Pt−OH adsorption or desorption (eq 1) are separated for more than 600 mV by the polarization barrier along the potential axis from the initial equilibrium potential of oxygen electrode, (1.29 V vs RHE) value of the ORR, when one implies the same pathway backward along the cathodic polarization scans (eq 2). In other words, both the energy chart diagram (Figure 1a) and the corresponding cyclic voltammograms (Figure 1b)[6] for the critical potential range reveal the absence of enough primary oxide spillover amounts necessary to speed-up the overall ORR, like within the Pt−OH adsorptive/desorptive potentiodynamic peaks, when the effective energy plateau establishes and grows. Namely, the reversible spillover Pt−OH generation (eq 1) then quickly ends-up with its highly irreversible one-way disproportionation consumption (eq 2), and becomes separated in both potential scan directions by the broad energy barrier in its anodic adsorptive growth and reversal cathodic desorptive removal. Thus, under such circumstances, the whole system is effectively missing enough starting amounts of the Pt−OH within the broader critical potential range to speed-up the entire backward ORR.

However, the entire cathodic ORR mechanism implies some fast consecutive reaction steps, including the primary oxide participation,[7]

$$O_2 + Pt + H_3O^+ + e^- \rightarrow Pt{-}OOH + H_2O(RDS) \quad (3a)$$

$$Pt{-}OOH + Pt \rightarrow Pt{-}OH + Pt{=}O \quad (3b)$$

$$Pt{-}OH + Pt{=}O + 3H_3O^+ + 3e^- \rightarrow 5H_2O + 2Pt \quad (3c)$$

and thereby provides one more substantial reason for the absence of any adsorptive accumulation of the Pt−OH upon catalytic Pt surface in the course of cathodic polarization. In such a respect, one of the fastest reaction steps in the overall ORR mechanism represents the self-catalytic interference of the Pt−OH spillover interplay with the Pt═O (eq 3c), and the present study might start from that point, while the latter has been the final consequence in the theory development and logically deserves and imposes such an actual and logical analytic display. Namely, such a kinetic reaction step implies a Pt−OH/Pt═O

dx.doi.org/10.1021/jp412292w | J. Phys. Chem. C XXXX, XXX, XXX−XXX

concentration ratio of about 1:1 to approach maximal reaction rates. The substantiation of such an idea implies interactive and optimized hypo-d-oxide catalytic support, which imposes hydroxide membrane transfer and requires continuous molecular water feeding supply within such a matrix, finally resulting in enriched Pt−OH storage and spillover all over the metallic Pt electrocatalytic surface[8−16] and all along the oxygen and hydrogen adsorptive and evolving limits. Meanwhile, in addition, one of decisive and conclusive kinetic and (electro)catalytic axioms would now be that the same intense spillover reacting species could by no means at the same time be both the participant of fast reaction steps and the rate determining species in the RDS.

In such a respect, it should also be noticeably observed that in both cathodic and anodic potentiodynamic scan directions, the reversible adsorptive and desorptive Pt−OH peaks precede or follow while mutually merging with the corresponding main growing and removing irreversible Pt═O peaks in all their cyclic voltammograms (like in Figure 1b).[2−5] In other words, in both cathodic and anodic scan issues, the Pt−OH plays the substantial self-catalytic initiating and stimulating promotion role, (eq 3c), along with the autocatalytic effect of water molecules,[17] for the interfering interplay in electrocatalysis with the Pt═O, finally yielding the optimized overall ORR. Merging peaks (*in* and *ex situ* XPS analysis[10,12,16]) are an *a priori* indication of the interference between two species, in particular since the interacting ones are distinguished one from another by the direct mutual recombination reaction (eq 2), and thence one notes their interdependent optimal ratio even at the topmost Pt═O desorption peak position in cyclic voltammetry. In such a context, the Pt−OH obviously takes place in all fast reaction steps within the overall mechanism of the ORR. In fact, the initial and the rate-determining state within the latter is effectively the Pt═O (eq 2), since all attempts to start the cathodic ORR with pure or plain Pt by the continuous mechanical abrasive grinding removal of its oxides, and this way exposing the clean metallic surface in aqueous media, failed to provide the reversible oxygen electrode behavior.[18] On the contrary, the exposed electrode surface by the autocatalytic effect of water molecules instantaneously becomes the monolayer Pt═O covered. Such potentiodynamic interference between the primary (Au−OH) and surface (Au═O) oxides becomes even more clearly delineated and marked by more pronounced corresponding merging peaks in cyclic voltammetry of gold electrocatalysts.[2−4] These, along with the causes and consequences associated with the primary oxide spillover phenomena, and thereby yielding distinct and pronounced dynamic catalytic improvements in the overall ORR kinetics and mechanism, will be now the main subject matter, guiding light motive, and leading idea of the entire present study. In fact, this is the first experimental evidence indicating that only the optimal interference between the reversible primary, Pt−OH, and unavoidable highly irreversible Pt═O, imposes such a distinct dynamic self-catalytic promotion and enables (even provides) the substantial overall electrocatalytic advances in the ORR. Since the electrocatalytic advances are clearly provided by the Pt−OH spillover effect, while the polarization obstacle imposes a much higher adsorptive strength of surface oxide (Pt═O), the overall idea for improvements toward the reversible ORR would consist in the latent storage and thereby enabled continuous spillover supply of the former all over the catalytic nanostructured Pt surface, regardless of the presence or absence of the latter.

In such a respect, the guiding concept implies homogeneous nanostructured distribution and selective grafting during interactive hypo-hyper-d-d-interelectronic bonding of Pt nanoclusters upon various mixed valence hypo-d-oxide supports, primarily Nb_2O_5,TiO_2 (or Ta_2O_5,TiO_2), because of their much advanced electronic conductivity. In such a constellation, nanoparticles of solid oxides and Pt establish the so-called SMSI (strong metal−support interaction),[8−13] the ones of strongest in the whole chemistry, together with the electron conductive transfer, while the surface of hypo-d-oxides undergoes spontaneous dissociative adsorption of water molecules and thereby becomes, along with continuous further water vapor supply, the undisturbed and almost unlimited latent storage and spillover source of the Pt−OH. The hypo-f-oxide doping and other secondary effects and specific contributions will be stepwise further displayed.

ELECTROCATALYTIC Pt═O/Pt−OH INTERFERENCE RATIO IN THE ORR

Let us now first consider polarization properties of typical and characteristic nanostructured electrocatalysts for the ORR, and select some diagnostic kinetic criteria revealed from their Tafel plots, to assess and compare their catalytic activity yielding therefrom: (i) Nanodispersed Pt clusters (10 wt % Pt) upon sol−gel developed indifferent nanoparticulate E-tek, Inc., Vulcan-XC-72 carbon (240 sq.m/g) carrier and current collecting species (Pt/C), considered now for the classical issue of such a comparison; (ii) The interactive supported nanostructured Pt particles upon highly stable and electron conductive (300−1000 S/cm) ceramic Magneli phases (Ebonex), $Ti_nO_{(2n-1)}$, on average Ti_4O_7, usually defined as a shared rutile structure, accommodating the oxygen suboxide deficiency in the structure by the formation of crystal shared planes along the *n*th layerlike plane of octahedron, so that Ti_4O_7 has one TiO for every three TiO_2 layers (Appendix in ref 8);[10] and (iii) Advanced interactive selective grafted and homogeneously dispersed Pt nanoclusters down to the prevailing (2.2 ± 0.1 nm) nanosize, upon the optimized structure of mixed valence hypo-d-oxide compounds (Pt/Nb_2O_5,TiO_2/C),[13,16] and even further extended (iv) composites with hypo-f-oxides (Pt/Nb_2O_5,CeO_2,TiO_2/C, including doped GdO_2, HoO_2, and LaO_2 itself), and their relative combinations. Such comparable diagnostic Tafel polarization interdependences are distinctly displayed in Figure 2, with differences of more than an order of magnitude in the electrocatalytic activity for the ORR that arise *only* as the result of different hypo-d-(f-)oxide type of interactive catalyst supports, relative ratios of their amounts versus metallic part of the catalyst (Pt), and their corresponding interactive (SMSI) bonding effects. It certainly would be worth noticing and inferring that almost the same electrocatalytic activity achievements (roughly 12:1, between interactive hypo-d-TaOx and even hypo-f-CeOx-oxide supported and nonsupported Pt/C) have recently been substantiated by Ohsaka et al.[19−23] and Mori et al.,[24−28] respectively. Thence, what are the causes for such coinciding consequences?

IRREVERSIBLE CAUSES, REVERSIBLE CONSEQUENCES, AND ELECTROCATALYTIC SPILLOVER ADVANCES FOR THE ORR

In such a respect, let us consider and compare some highly corresponding subtle and characteristic complementary potentiodynamic events, and the revealing appearances therefrom.

dx.doi.org/10.1021/jp412292w | J. Phys. Chem. C XXXX, XXX, XXX−XXX

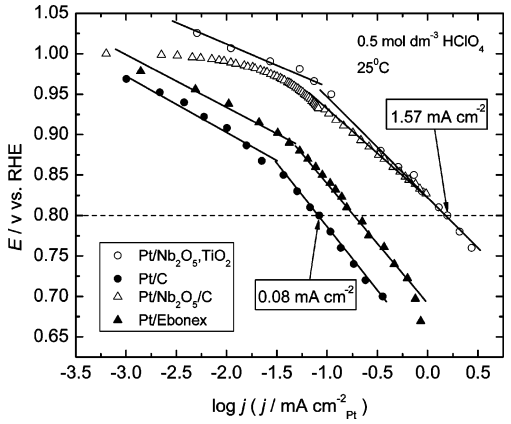

Figure 2. Tafel plots for the cathodic ORR scanned on RDE in 0.5 M $HClO_4$ solution at 25 °C for E-tek, Inc., Pt/C (Vulcan XP-72, closed circles); Pt/Ebonex (Magneli phases, closed triangles); Pt (10 wt %)/Nb_2O_5 (20 wt.%)/C (70 wt.%) (open triangles); and Pt/Nb_2O_5 (5 mol.%), TiO_2 (95 mol.%) (open circles).

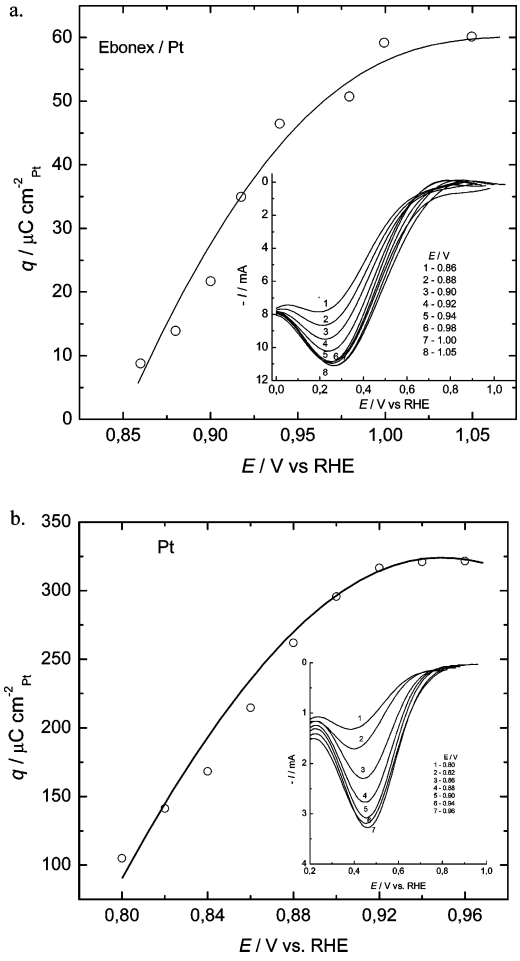

Figure 3. (a) Charge density (q) that requires adsorbed oxygen species for their reduction, presented as a function of potential for Pt/(Magneli phases) (5 mg) electrode, as in Figure 2. The inset shows potentiodynamic I vs E relations scanned from indicated different initial potentials (hold) with a sweep rate of 5 $V{\cdot}s^{-1}$. (b) The same as panel a, but for polycrystalline Pt metal.

Substantial interest is now primarily focused on the actual mixed interfering Pt oxide coverages at various points within the characteristic potentials close to the open circuit value and mostly along the reversible potential range of low Tafel line slopes (mostly about 30 mV/dec). In such a respect, each of the preconditioned electrodes at 0.20 V (RHE) was then successively potentiostated at all these selected potential values (Figure 3a,b), for a fixed time period (30 s), and afterward, to avoid and mask all slow reaction steps, being further exposed to the high sweep rates in the striping voltammetry scans, from such selected initial values down to 0.0 V (RHE) (Figure 3a,b, insets). The main withdrawn potentiodynamic conclusion of general fundamental significance has then been that all along the reversible Tafel range, Pt electrodes, plain and interactively supported upon hypo-d-oxides, have been covered by various, but prevailingly Pt═O/Pt−OH mixed Pt oxide layers, while at higher irreversible polarization (120 mV/dec), these were completely deprived from such adsorptive deposits. In other words, while within the reversible range of low Tafel line slopes, the ORR proceeds upon mixed oxide covered Pt surfaces, as the interfering self-catalytic spillover electrode process (eq 3c)—like at its open circuit potential, the plain Pt surface is perfectly cleaned from its oxides and requires imposing much higher polarization for the same reaction to occur. In fact, *vice versa*, the remarkably higher polarization in the ORR implies complete Pt-oxide consumption and fully deprived Pt surface from any coverage. This means that in the absence of the primary (Pt−OH) versus surface (Pt═O) oxide coexistence at the Pt electrocatalyst surface, the cathodic ORR imposes and requires remarkable polarization to take place. In fact, contrary to the spontaneous adsorptive hydrogen adatoms (Pt−H) deposition, and that way establishing the corresponding reversible hydrogen electrode properties with thermodynamic equilibrium potential value (0.0000 V vs. RHE), so far there is no reversible oxygen electrode when Pt becomes entirely deprived from its primary, in conjunction with the surface oxide.[18] On the contrary, the Pt surface, fully deprived of its oxides, first of all from the Pt−OH, imposes and implies rather high electrode polarization for the ORR. Just like the Pt(H_2)/Pt−H/H_3O^+ reversible equilibrium for hydrogen electrode, its oxygen counterpart requires and implies some similar and corresponding thermodynamic relation (Pt(O_2)/Pt−OH,Pt═O/OH^-) to approach the reversible oxygen electrode with both firm and reproducible thermodynamic potential value (1.29V vs RHE), and reversible behavior within the remarkably extended reversible Tafel potential range and along the broader potential axis. The problem and obstacle are the initially highly polarizable monolayered Pt═O, and at the same time the missing Pt−OH species, these being far interseparated within the critical range one from another along the potential axis (Figure 1a,b). Thence, the Pt−OH, in conjunction with Pt═O, plays the same substantial and decisive role for the ROE, as H-adatoms (Pt−H) do for the RHE, and this is diagnostically clear from classical cyclic voltammograms. Such experimental evidence logically imposes the leading idea to approach and create the ROE properties and features by the continuous interfering Pt−OH versus Pt═O relation and interplay, as otherwise already revealed and established from the initial reversible Tafel line plots, and to now become extended all along to and from the oxygen evolving potential limits.

The amount of charge (Figure 3a,b) imposed during such scans, and determined by their peak integration, proved that the surface coverage of Pt interactive supported on Magneli phases (Pt/Ti_4O_7) by adsorptive oxide species was by an order of magnitude lower than on nanostructured, but noninteractive supported Pt/C, because of the remarkably higher catalytic

dx.doi.org/10.1021/jp412292w | J. Phys. Chem. C XXXX, XXX, XXX−XXX

activity and/or distinctly increased reaction rate at the same potential values, and both were decreasing with successive negative potential values of polarization, the adsorption conditions being Langmuirian in all issues. These rather specific potentiodynamic measurements even more clearly and convincingly show that the cathodic ORR upon Pt/Ebonex starts and finishes at remarkably and distinctly more positive potential values (1.05 down to 0.86 V, versus 0.95 down to 0.8 V, all versus the RHE), relative to polycrystalline Pt metal and/or nanostructured Pt/C; two other congenial issues (iii and iv) initiate with 1.29 V as the completed reversible property of the ROE (see Figures 6 and 7 below). In such a respect, the interactive hypo-d-oxide support of the Pt electrocatalyst apparently has and imposes remarkable advantages of fundamental significance in (electro)catalysis by its induced spillover of the primary oxide (Pt−OH). The higher the altervalent capacity of the interactive hypo-d-oxide support or mixed valence compound, under optimal wetness conditions, the more pronounced results of the entire interfering Pt−OH/Pt═O catalytic effect. In the same way, the higher the specific ratio between the amount (or exposed surface) of such mixed valence compounds (or even the individual hypo-d-oxide) versus the exposed active Pt catalytic surface, or the higher the latent primary oxide storage accumulation (and thereby the spillover feeding effect, see Figure 7 below), the higher the resulting overall spillover rate and electrocatalytic effect of Pt−OH (or, in general, M−OH) on the ORR. Consequently, thence the interplay (and/or the interference) between the reversible primary (Pt−OH), and polarizing surface (Pt═O) oxide, clearly shifts the upper initial potential for the ORR to substantially more positive values, and in such a manner reveals and traces the path toward the electrocatalyst of the reversible oxygen electrode (ROE) properties. Even more so, by such a dynamic electrocatalytic effect, the the whole reaction rate of the cathodic oxygen reduction remarkably increases. The same corresponding initial potential shift toward more positive cathodic values has also recently been recorded both on Pt/TaO_x[19−23] and Pt/CeO_x[24−28] interactive (SMSI) supported and remarkably advanced electrocatalysts in their catalytic activity for the ORR.

THE SELF-CATALYTIC MOLECULAR WATER EFFECT

In the same sense, Ertl et al.[17] have additionally shown and experimentally proved by HREEL spectra along with STM images that the Doebereiner catalytic reaction of hydrogen oxidation upon Pt surface, even at low temperatures (140 K), proceeds with remarkable amounts of the primary oxide (labeled as OH_{ads}), as the decisive and accumulated intermediate, including the auto- or self-catalytic step with adsorbed water molecules,

$$O_{ads} + H_2O_{ads} \rightarrow 2OH_{ads} \quad (4a)$$

or, in the equivalent system of the present study,

$$2Pt + O_{ads} + H_2O_{ads} \rightarrow 2Pt{-}OH \quad (4b)$$

In fact, Ertl has pointed out the substantial autocatalytic role and the pronounced overall significance of water molecules in heterogeneous catalysis for oxidation processes that generally proceed over the Pt−OH generation and spillover. The present study in the same sense reveals the increase of the overall reversible reaction rate of the Pt−OH generation (eq 1), and its further undisturbed spillover, both caused by the pronounced and decisive effect of polarized water dipoles within the double layer,[29] and the polarization itself as the stimulating driving force. Namely, in such a sense, the latter (eq 1), represents the electrochemical and electrocatalytic equivalent to the Ertl mechanism (eqs 4a and 4b) in heterogeneous catalysis. In fact, as already pointed out above, in the electrochemical sciences, it is well known from cyclic voltammograms scanned on Pt and Au[2−6] that both the anodic adsorptive primary oxide growth and its cathodic desorption proceed as highly reversible and thereby extremely fast electrode processes. In principle, such typical dipoles (M−OH) are 1:1 employed and present within the broader potential range for the double-layer capacitor charging and discharging,[8−16] and this is proved by the corresponding symmetric and highly reversible potentiodynamic peaks of the interactive supported electrocatalysts (Figure 6, below).

As concerns the H-adatom spillover yielding the bronze state ($Pt/H_{0.35}WO_3$) out of preceding hydrated species, Tseung et al.[30−32] much earlier achieved the same bronze type electrocatalysts and corresponding remarkable catalytic results along the developed phase, both with micro- and macro-structured Pt electrodes interactively substantiated in the same polytungstic environment, as a hint for and the forerunners to the advanced novel nanostructured interactive supported (SMSI) bifunctional electrocatalysts, while the definition of the bronze properties originate from Glemser and Naumann.[33]

In the same sense and context, it would be worthwhile to observe continuously growing similar and congenial trends and corresponding achievements with various interactive hypo-d-oxide-supported electrocatalysts primarily based on the Pt−OH spillover effect;[34−49] the difference in the theory consists only in the Pt−OH spillover direction.[8−16,19−28]

Finally, the same interactive (SMSI) type of mixed-altervalent hypo-d-oxides primarily based on NbO_x and TaO_x supports are compatible with and most promising for photoelectrocatalysis, and mainly for cathodic hydrogen (HER) and anodic oxygen (OER) evolution reactions.[50−55] In such a respect, the whole advancing composite and combined photo- and elecro-catalytic effect again originates and comes from both the spillover of H-adatoms in the HER and primary oxides (M−OH) for the OER, and in this way reveal their broader and even universal sense and significance.

PRIMARY OXIDE SPILLOVER AND INTERRELATED ANODIC HCHO OXIDATION

Cyclic voltammetry has been employed to investigate and characterize the potential dependent growing adsorptive anodic and reverse desorptive cathodic Pt−OH surface properties, because potentiodynamic spectra afford the most illustrative, versatile, and reliable scanning method for studies of fast heterogeneous electrode reactions in aqueous media all along the potential axis between hydrogen and oxygen evolving limits. Since the heterogeneous reaction of formaldehyde oxidation with Pt−OH, and in particular Au−OH, proceeds as a fast reversible anodic, mass transfer limited process, and since HCHO is soluble in all ratios in aqueous media, the primary oxide generation rate and its yielding spillover have primarily been investigated by potentiodynamic spectra within the broader concentration range (Figure 4a,b).[8,10,13,56] Namely, it has then been unequivocally shown that for an order of magnitude higher HCHO content, there are correspondingly increased limiting current values of its anodic oxidation, or corresponding peak values in the present cyclic voltammogram spectra (Figure 4a,b).[8−11,13,56]

Such an order faster heterogeneous reaction of anodic HCHO oxidation is apparently able to postpone, within an unusually broad potential range, the recombination of the Pt−OH (eq 2)

dx.doi.org/10.1021/jp412292w | J. Phys. Chem. C XXXX, XXX, XXX−XXX

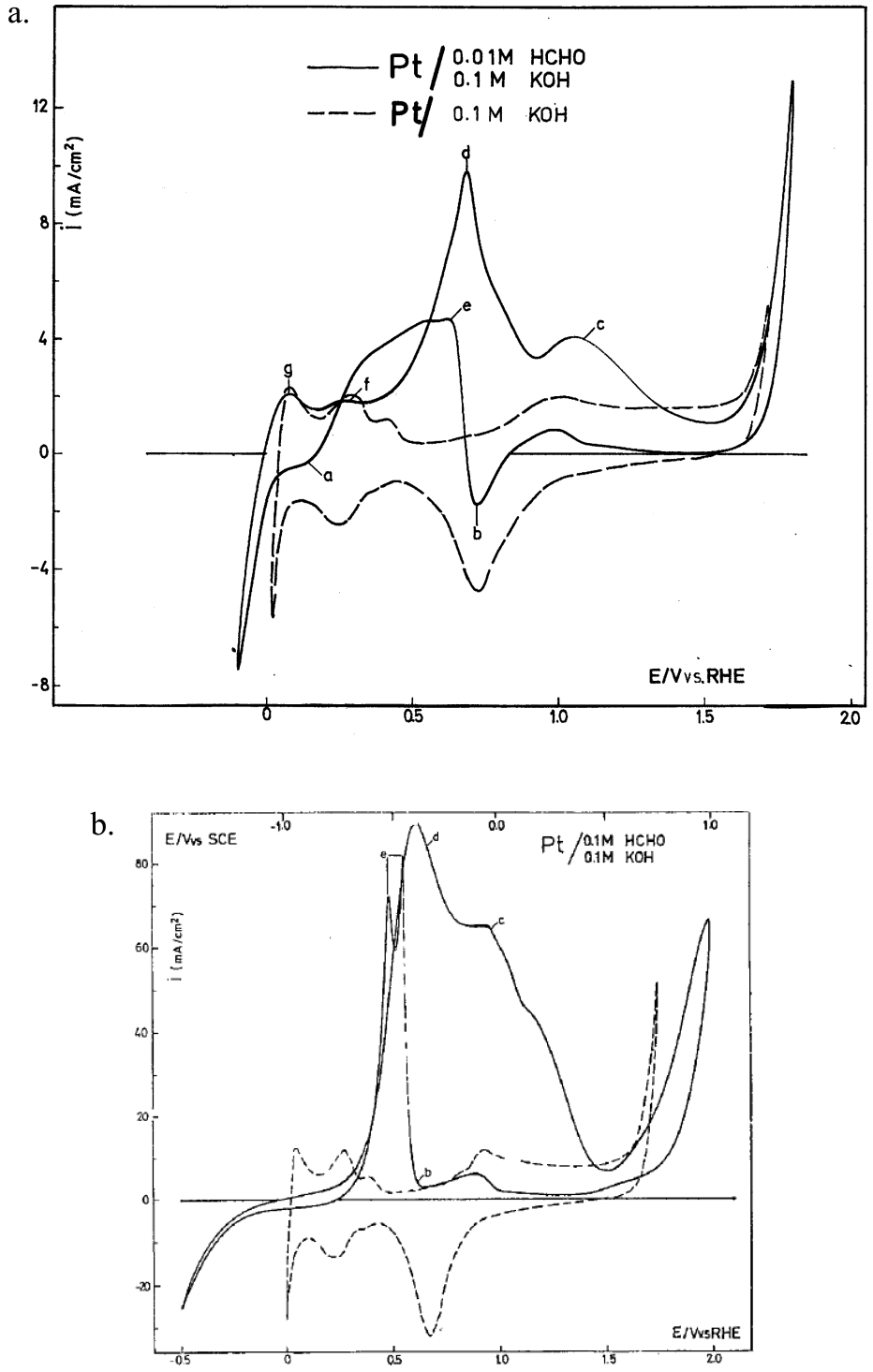

Figure 4. (a,b) Cyclic voltammograms scanned on a polycrystalline Pt wire electrode in alkaline (0.1 M KOH, dashed lines) solution and in an admixture of formaldehyde (0.01 M (a) and 0.1 M HCHO (b), solid lines) at a 200 $mV \cdot s^{-1}$ sweep rate between hydrogen and oxygen potential evolving limits. Labels: (a) reversible hydrogen adsorption peak; (b) irreversible Pt surface oxide (Pt═O) desorption peak; (c,d) successive peaks of anodic aldehyde oxidation; (e) sudden sharp current jump and reverse peak of repeated HCHO oxidation in the course of successive cathodic scan; (g,f) reversible H-adatoms oxidation and desorption peaks, respectively.

into the more polarizable, more adsorptive, and more stable Pt═O.

The enriched potentiodynamic experimental evidence,[8−11,13−16,56] in accordance with the theory of instantaneous reversibly revertible alterpolar properties of the bronze type electrocatalysts,[13−16] and extremely broad potential range of the primary oxide adsorption and desorption, unambiguously testify now that the Pt−OH (AuOH, M−OH) in all circumstances in aqueous media both underpotential deposition (UPD) and overpotential desorption (OPD) charges and discharges DL (double layer), (eq 1), and thence is available for reaction all along within such extended potential limits. For example, formaldehyde oxidation starts exactly at its reversible potential value (0.32 V vs RHE), at the usual lower DL charging potential

dx.doi.org/10.1021/jp412292w | J. Phys. Chem. C XXXX, XXX, XXX−XXX

limits, even merges with the second UPD desorption peak of H-adatoms, and extends as a rather exaggerated broad twin peak all along the anodic scan, just until the beginning of OER (Figure 4a). In the same sense that anodic striping CO oxidation on composite hypo-d-oxides supported Pt or Pt, Ru catalysts take place even within the usual interval of H-adatoms desorption and can even be brought with the reversible composite altervalent and mixed valence bronze type Pt electrocatalysts (Pt/Nb_2O_5,TiO_2/C or even Pt/Nb_2O_5,TiO_2 and Pt/Ta_2O_5,TiO_2/C), under the conditions to be initiated just above the HER (nearly at 0.0 V vs. RHE). In other words, Pt−OH becomes available for reaction not only within its nominal reversible adsorption and desorption peak limits in regular mineral acid or base aqueous solutions,[2−5] but depending on the reactant (HCHO, CH_3OH, HCOOH, etc.) concentration, affinity, and its actual reaction rate, along an unusually broad and extendable potential range, similarly as and in accordance with the DL capacity charging/discharging extends along the potential axis.[8,10−13] Even more so, the interactive hypo-d-oxide catalyst supports, depending both on their specific amount per projected area and individual or mixed valence composites, are available for further dramatic potentiodynamic peak extensions.[19,20]

Plentiful potentiodynamic experimental evidence testifies that whenever there exists enough supply of some species of rather fast oxidation ability, being much faster (more than an order of magnitude) than the next step of M−OH recombination transfer into the rather stable (strong adsorptive or highly polarizable) M═O growing monolayer, (eq 2), such as various aldehydes and simple alcohols, and even various monosaccharides,[56] their anodic reaction starts immediately after (or even within) UPD H-adatom desorption,

$$R{-}CHO + M{-}OH + H_2O \rightarrow R{-}COOH + M + H_3O^+ + e^- \quad (5)$$

and proceeds further all along the DL charging/discharging capacity range in acidic or alkaline solutions. Such a rather broader charge capacity area (Figure 4a,b), usually features all the properties of typical underpotential oxidation (UPO) and deposition (UPD) peaks,[10−12] in particular when compared with cathodic UPD and anodic OPD peak properties of H-adatoms on various metals.

Stepwise potential extension of positive potential limits toward the oxygen evolution clearly shows (Figure 4a,b) the absence of surface oxide growth almost until oxygen starts evolving. Thus, since during the reverse potential scan toward the HER there correspondingly arises Pt═O desorption much earlier and of dramatically smaller charge capacity than in the simple acidic or alkaline solutions, the appearance of a characteristic sharp anodic current jump testifies of the repeated or hysteretic aldehyde oxidation even within the cathodic or former DL discharging range. This is the first evidence of hysteresis in cyclic voltammetry and reflects the specific and highly reactive properties of the Pt−OH, and deserves some impact observations. In fact, the point and substance are that the repeated *anodic peak* evolves and extends in the course of *cathodic scan* direction, and thence becomes hysteresis. Such unusual behavior testifies that Pt−OH (Au−OH) features absolutely equal abilities as concerns cathodic and/or anodic reaction, just as the reaction complexes can and do while at the top of energy barrier, and this can be concluded from the reversible primary oxide ideal adsorption and desorption peaks. In other words, the fastest of available reactions then decides as concerns the peak growth and direction, and this is a pronounced unique property of primary oxide species. The competition takes place between anodic HCHO oxidation to produce HCOOH and cathodic reduction yielding H_2COH—the reaction rate order being about 15:1—and in this way settling things down and convincing.

Such state of plentiful (no exception) experimental potentiodynamic evidence[10−12,56] imposes some outstanding observations and conclusions:

There is no aldehyde or alcohol anodic oxidation upon the M═O-covered metal prior to the potential of molecular oxygen evolution, just as the recombination transfer of M−OH into the Pt═O adsorption layer becomes prevented as long as the oxidation of rather more reactive species of aldehyde remarkably exceeds such a "degradation" of an active (M−OH) into rather passive (M═O) species. This implies that there is no anodic OER, as long as the (minimal) critical (M═O) surface oxide coverage is absent. As a corollary, there is no anodic aldehyde, alcohol, their simple acids, and even CO oxidation upon Pt═O covered surface, but only upon prevailing Pt−OH amounts.

Such pronounced potentiodynamic features of enormous growing HCHO anodic oxidation peaks impose some far-reaching conclusions for the present study. Namely, since aldehydes are often soluble in aqueous media in almost all ratios, their voltammograms at high contents feature extremely high imprinted charge capacities and limiting current values at their peaks, and thereby testify of the almost unlimited reversible reaction rate (eq 1), as long as diffusional mass-transfer supply provides enough reacting species. This is even more so for interactive supported Pt and Au upon high altervalent hypo-d-oxides and their mixed valence compounds, since these behave as the highly enriched latent storage Pt−OH spillover sources.[8−16,19−28] This is the cause and reason why, within the reversible part of Tafel plots, the electrocatalytic metal (Pt,Au) surface is always covered by the interacting primary and surface oxides and naturally tends to impose the ROE properties.

Meanwhile, in such a context one of the most outstanding observations has then been that cyclic voltammograms of both formaldehyde (Figure 3, ref 19) and formic (muriatic) acid (Figure 3, ref 20) anodic oxidation distinctly differ upon plain (Pt/C) and the same but interactive supported hypo-d-oxide (Pt/Ta_2O_5/C). In other words, all parameters and conditions being the same, the reaction rates become dramatically different upon supported versus nonsupported electrocatalysts, as the result of the distinctly different additional Pt−OH spillover feeding effect and as the only distinctly imposed difference. Such a conclusive observation belongs to the main experimental arguments to prove the theory of the M−OH interfering self-catalytic spillover contributions in electrocatalysis of aqueous media, finally providing the electrocatalysts with the ROE behavior and properties, and enlightening the way and entire approach for its substantiation.

Any assumption that there might be a fast direct electron exchange electrode reaction, instead of aldehyde oxidation by the M−OH, could not find stable ground. Namely, then Pt would be much more active than Au, while plentiful potentiodynamic evidence proves otherwise, just because their various surface oxides feature much different adsorption strengths. In such a context, it would be worth mentioning that the same and rather pronounced potentiodynamic results of the Pt−OH spillover effect were obtained by Tseung et al.[57] with D-glucose oxidation upon a specific electrode deposit cathodically produced by codeposition of Pt/WO_3 from tungstic acid solution (Figure 1, ref 57). The latter probably was WPt_3 upon a WO_3 support, also

dx.doi.org/10.1021/jp412292w | J. Phys. Chem. C XXXX, XXX, XXX−XXX

adjoined upon basic Pt/WO_3 substrate, though the authors name it the "precious metal/hydrogen bronze anode catalyst" and simply label it as Pt/WO_3.[30−32]

SPILLOVER PHENOMENA: CAUSES AND CONSEQUENCES

Spillover phenomena in heterogeneous catalysis and electrocatalysis usually arise and reflect as strong repulsion forces, when the ionic species of the most fast reaction step partially transfer their charge to the interacting catalyst surface and become spillover dipole intermediates (Scheme 1). The driving force for such effusion effects imposes the gradient of electrochemical potential that implies chemical potential for heterogeneous catalytic processes, so that some specific ionic species undergo migration over or within some solid state electrolytic matrix that exhibits membrane transferring properties, and finally emerge upon the exposed electrocatalyst surface as the spillover dipoles, (eq 1).

Spillover phenomena impose advanced electrocatalytic effects on and play a significant kinetic enhancement role in various electrochemical processes, in particular for the oxygen and hydrogen electrode reactions.[8−16,19−28] Namely, the fundamental Guldberg-Waage law of mass action (1865−1879)[58] predicts that the faster the spillover effect of the reacting intermediate species, the more enhanced the corresponding electrode reaction becomes. Since all electrode processes belong to heterogeneous electrocatalytic reactions, almost unlimited spillover intensities certainly succeed to enhance and speed up the overall reaction rate much more than any ionic solubility amount for mass transfer limited electrode reactions occurring from and in electrolytes. Then, what would be the main prerequisites for proper spillover features to be imposed to occur in electrocatalytic processes in aqueous media?

The first decisive step toward rather fast spillover expanding phenomena of the primary oxide (M−OH) has been the consequence of a strong first-principle thermodynamic confirmed evidence (density functional calculations, DFC) by Vittadini et al.,[59] that water molecules undergo prevailing (for more than 50% of the entire available surface) spontaneous dissociative adsorption on anatase and even rutile titania, and more so on the higher altervalent oxides[60] of tungsten, molybdenum, tantalum, niobium, and/or cerium, etc. (Figure 5). In addition, the first-principles molecular-dynamic simulations showed the existence of a mechanism for thermodynamically favored spontaneous dissociation of water molecules even at low coverage of oxygen vacancies of the anatase (101) surface,[61] and consequently to the Magneli phases ($Ti_nO_{(2n-1)}$, on average Ti_4O_7), as substantially suboxide structure, otherwise significant both as highly bulk electronic conductive,[8−11,13] membrane type surface transferring hydroxide species and interactive catalyst support. In fact, this is the status of reversible open circuit dissociative adsorption of water molecules at the equilibrium state, something like capillary phenomena in adsorption after some critical coverage extents. Meanwhile, in the presence of the nanosized metallic part of the catalyst, and continuous enough moisture supply (Boudart et al.[62−65]), directional electric field (or, electrode polarization), further disturbs such an established equilibrium and dynamically imposes further continuous forced dissociation of water molecules, and as a consequence, their membrane transport properties (Livage et al.[66−68]), and the resulting spillover features.[8−11,13−16]

Heterogeneous catalysis broadly employs the Tauster[69−72] SMSI (strong metal−support interaction) effect to increase the overall catalytic activity, but so far the additional interactive spillover contribution of the M−OH, in particular for the catalytic oxidation processes, has not been noticed and/nor considered, while being clearly implied under a broader term and meaning of oxidation itself. However, heterogeneous catalysis does not employ anodic polarization, except for the electrochemical promotion of catalysts (EPOC, NEMCA), and then it never experiences, nor investigates the M−OH spillover.

The point is that even under the wet state, the internal bulk keeps its initial solid oxide structure and corresponding electronic conductivity, in particular under the strong (SMSI) hypo-hyper-d-d-interelectronic bonding (Pt/Nb_2O_5), and the growth of reinforcing intermetallic phases ($NbPt_3$) in between at

Scheme 1. Model Presentation for the SMSI Effect[a]

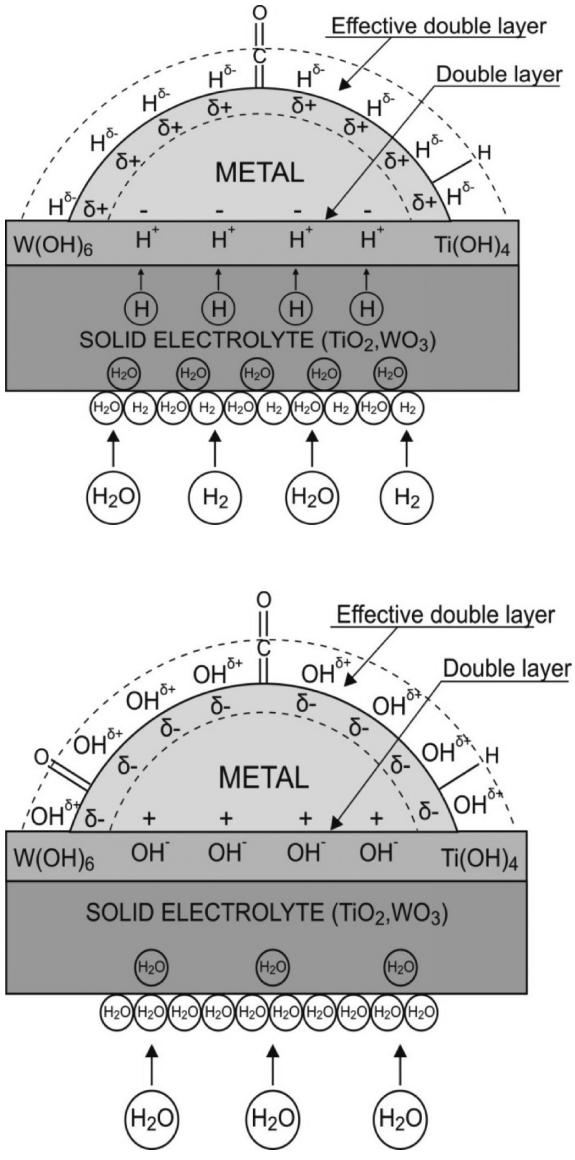

[a]This results in the spillover transfer of H-adatoms within the bronze nanostructure ($Pt/H_{0.35}WO_3$, a), and/or the primary oxide (M−OH) effusion, as a dipole along the hydrated counterpart ($Pt/W(OH)_6$, b), further continuously transferring them upon the metallic part (Pt) of catalyst; otherwise both originating from the hypo-d-oxide continuously fed by a moisture stream to such a composite ($M/TiO_2,WO_3$) electrocatalyst structure and maintaining them in the reversible interchangeable equilibrium ($Pt/H_{0.35}WO_3 \leftrightarrow Pt/W(OH)_6$), (constructed by Dimitris Tsiplakides).

dx.doi.org/10.1021/jp412292w | J. Phys. Chem. C XXXX, XXX, XXX−XXX

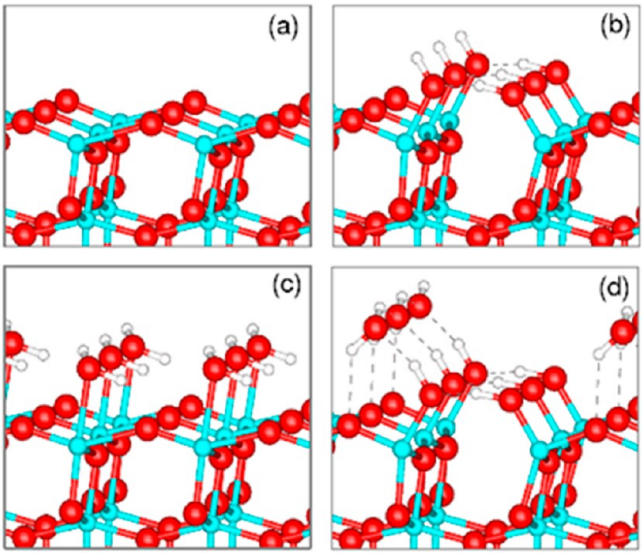

Figure 5. The perspective views of DFT-optimized atomic structures for (a) the clean anatase (ADM) ad-molecule model of unreconstructed (001) surface; (b) the dissociated state of water (0.5 monolayer) on (001); (c) the relaxed geometries of molecular state of adsorbed water (1.0 monolayer of hydroxylated anatase) on (001); and (d) the mixed state of water on (001) with a half-dissociated coverage of adsorbed monolayer water molecules (courtesy by A. Vittadini, cf. ref 59).

the interface. The latter then keeps the composed solid structure ($Pt/NbPt_3/Nb_2O_5$) as a rather homogeneous and reinforced strong unit body. In other words, the d-band is cohesive, adsorptive, surface free, and thereby the most decisive catalytic and electrocatalytic orbital, while hyper-hypo-d-d-interactions and bonds belong to the strongest in the entire chemical sciences ($HfPd_3$, as an extreme, reacts vigorously explosive).[73] Meanwhile, the dissociative water adsorption makes surface and porous oxide structure interchanged into hydroxide structure ($Nb_2O_5 \rightarrow 2\ Nb(OH)_5$), and now ready for membrane type transport, finally yielding the partial electron transfer to the metallic part of the electrocatalyst (Pt) that then imposes the Pt−OH spillover. Such state of the art is essentially why Boudart[62−65] then requires at least a monolayer of capillary water adsorptive deposit, to initiate and enable rather fast both cathodic H-adatoms and, in particular, anodic the Pt−OH spillover. This is also the reason why along with the increased hypo-d-(f)-oxide bulk, there correspondingly grows its exposed surface, and as the overall yield, extends the latent 'storage' of the primary oxide for its subsequent electrocatalytic spillover widespreading. Meanwhile, the latter is not unlimited appearance, but passes over well-defined maximum of tremendously high values (Figure 11, ref 74). In such a respect, the most privileged hypo-d-oxide state belongs to Nb_2O_5 and Ta_2O_5 in combination with TiO_2.

The first spillover phenomenon in heterogeneous catalysis was observed and defined by Boudart[62−65] for the interactive supported bronze type (Pt/WO_3) catalyst, initially at high temperature (above 400 °C) for pure solid system. Meanwhile, after the dissociative adsorption of water molecules on hypo-d-oxide support of Pt, the fast interactive effusion of H-adatoms over its hydrated ($W(OH)_6$) surface becomes dramatically sped up, even at ambient conditions in the ultimate presence of condensed at least monolayered aqueous precipitate,[62−65] establishing capillary phenomena of speeding up effusion of catalytic reaction intermediates (Pt−OH, Pt−H). Such a striking sharp wetness impact upon the overall spillover phenomena associated with hydrated hypo-d-oxides in aqueous media clearly implies Ertl[17] autocatalytic molecular water effect. This is significant for both the evidence of the extremely fast spillover widespreading migration and the resulting imposed reversible substrate reduction. The latter finally leads to the corresponding form of electrocatalytically active bronze ($Pt/H_{0.35}WO_3$) for cathodic processes, in which nonstoichiometric incorporated hydrogen obeys the same free reactive properties like adsorptive H-adatoms, and is the main source for the electrode or heterogeneous catalytic reaction. In other words, the point is that spontaneous dissociative adsorption of water molecules[59−61] imposes much smaller activation energy for transformation of the resulting hydrated $W(OH)_6$, into the corresponding bronze state ($Pt/H_{0.35}WO_3$), occurs even at ambient temperature, then behaves remarkably different than the initial dry oxide WO_3, and thereby, dramatically facilitates the overall spillover effect under pronounced wet status (the activation energies thence being in the ratio of 2.2, one with another, $WO_3 \rightarrow W(OH)_6$). The alterpolar interchanges between the bronze type electrocatalyst and its hydrated state ($Pt/H_{0.35}WO_3 \leftrightarrow Pt/W(OH)_6$) are correspondingly approved occurring instantaneously and reversibly fast, exactly because of the advanced and sped Boudart[62−65] spillover effect.

For the present study, it is of the same significance to notice and discuss the dissociative hydrogen adsorption followed by fast spillover, establishing in this way the storage capacity of H-adatoms on the wet sol−gel developed surface of carbon current collecting electrocatalysts support (like E-tek Vulcan XC-72), in particular facilitated by the metallic part of catalyst,[75−78] and the hydrated hypo-d-oxide support.[8−16] *Ab initio* molecular orbital studies have shown that adsorption of H-adatoms on the graphite basal plane[76] is an exothermic process. As a consequence, hydrogen spillover implies the transfer of electrons to acceptors within the support, in this way modifying the chemical nature of the latter, activating previously inactive substrate and inducing H-adatoms spillover sorption like laterally widespread expanding mobile repulsive dipoles.[75,76] In such a way, oxygen functional groups usually facilitate H-adatoms spillover and their reductive interaction (rough value 1,200 mol/cm^2/s, with linear velocities of 100 cm/s at edges of Pt crystallites, reducing down to a still high value of 5 cm/s midway between Pt particles, or for about 8 to even 9 orders of magnitude amounting the transferring distance relative to the radius of spillover dispersing species), so that the formation of Mo-bronze is an even faster process relative to tungsten.[76] The fascinating fact is that such spillover transferring rates are obtained within mild pH conditions and even upon mild hydroxide species, far from concentrated phosphoric acid of contemporary PEMs for actual and prospective fuel cells. Even more so, primary oxides adsorb homogeneously upon exposed sol−gel developed carbon nanoparticles surface, but do not impose any (MS controlled) noticeable oxidation. Such an adsorptive spillover effect of H-adatoms for bronze type electrocatalysts, and *vice versa*, for the equivalent Pt−OH effusion, and their mutual reversible alterpolar interchanges, correspond to the fastest known chemical reactions.

MEMBRANE PROPERTIES OF HYPO-D-OXIDES

Hypo-d-electronic transition metal oxides usually feature several altervalent states giving rise even to interactive mixed valence compounds, such as, for example, TiO_2/WO_3, TiO_2/Nb_2O_5, TiO_2/Ta_2O_5, or $TiO_2/Nb_2O_5/CeO_2$, and then correspondingly increase the overall spillover effect of both H-adatoms and primary oxides. Such an oxide network, in particular of polyvalent

dx.doi.org/10.1021/jp412292w | J. Phys. Chem. C XXXX, XXX, XXX−XXX

(high altervalent capacity) hypo-d-elements, when in hydrous state, behaves as an ion exchange membrane.[66−68] In fact, gels (aero and xerogels) are biphasic systems in which solvent molecules are trapped inside an oxide network, and such a material can be considered as a water-oxide membrane composite.[66−68]

Such a membrane transferring mechanism first implies the spontaneous dissociative adsorption of water molecules (eq 1a),[59−61] as long as enough moisture supply[62−65] enables its continuous occurrence, immediately followed by the hypo-d-oxide membrane transfer (eq 1b and 1c) that proceeds under anodic polarization,[10,11,16,59−61] and finally results with partial electron transfer to the metallic part of electrocatalyst and spillover of the M−OH, (eq 1), all over its exposed electrode surface, as dipoles Pt−OH (Scheme 1), which for Nb_2O_5 means,

$$Nb_2O_5 + 5H_2O \leftrightarrow 2Nb(OH)_5 \quad (1a)$$

$$Nb(OH)_5 + M \rightarrow Nb(OH)_4^+ + M{-}OH + e^- \quad (1b)$$

$$Nb(OH)_4^+ + 2H_2O \rightarrow Nb(OH)_5 + H_3O^+ \quad (1c)$$

$$\sum M + 2H_2O \leftrightarrow M{-}OH + H_3O^+ + e^- \quad (1')$$

The interchangeable mechanism in this way implies and imposes the anodic OH^--transfer within and prevailingly over the exposed surface of such ion exchange membrane, yielding the consequent spillover of the interactive M−OH dipoles all over the metallic catalyst particles (Scheme 1).[2−5] Alternatively, cathodic spillover of H-adatoms exerts spontaneous reduction of hydrous niobium oxide into corresponding bronze ($Pt/H_xNb_2O_5$).[8−11,13−16] These two spillover processes are fast and reversible,[13−16] so that every change of catalyst polarity imposes instantaneous altering of Nb-bronze into its hydrated oxide ($Nb(OH)_5$),[8−11,13−16] ($Pt/H_xNb_2O_5 \leftrightarrow Pt/Nb(OH)_5$), and *vice versa*, so that such an equilibrium has typical and substantial thermodynamic sense and meaning.

The problem so far was in unattainable nanostructured Pt-bronze, the catalytic activity of which exponentially increases with decreased Pt nanosize approaching maximum at monatomic dispersion (Mavrikakis et al.[79]). This requirement has now been fulfilled by the grafting implementation of Pt-acac (Pt-acetylacetonate) within colloidal particles of peroxopolytungstic acid, niobia (Nb_2O_5), tantalia (Ta_2O_5), and ceria (CeO_2).[8−16,19−28] Concerning the H-adatoms spillover yielding the bronze state out of preceding hydrated species, Tseung[30−32] has achieved correspondingly the same results even with micro- and macro-structured Pt electrode in the same polytungstic environment.

POTENTIODYNAMIC SCANS OF THE PRIMARY OXIDE SPILLOVER AND EXTENSION OF REVERSIBLE PROPERTIES FOR THE ORR

The first experimental evidence for the fast reversible anodic adsorptive growth and corresponding cathodic desorption of the Au−OH and Pt−OH, and thereby for their electrochemical spillover confirmation is primarily owed to the excellent potentiodynamic spectra of Conway et al.[2−5] (cf. ref 6). The former by their coinciding positions along the potential axis reveal the typical double layer charging and discharging features of dipolar species upon and from a capacitor. In the same sense, cyclic voltammetry has now primarily been recalled to scan the enriched (intensified) hydroxide ions membrane transferring effect, enabled by continuous moisture saturation feeding supply of the hypo-d-oxide support structure of composite nano-structured electrocatalysts,[62−65] upon the whole reinforced Pt−OH both chemisorptive generation and desorptive removal, and consequently, to record its spillover dynamics while charging and discharging of the DL capacity.[8−16,47,49] The same growing spillover contribution as a function of an extended specific amount of hypo-d-oxides on the resulting latent Pt−OH storage enlargement has been confirmed by Ohsaka et al.,[19−23] while Mori[24−28] obtained similar results with hypo-f-oxide support.

In this respect, an intermolecular compatible hypo-d-oxide composite mixed valence architecture (5.0 mol % WO_3, 95.0 mol % TiO_2 = 20 wt %, along with 10.0 mol % Nb_2O_5, 90.0 mol % TiO_2 = 20 wt %), as the interactive catalytic sub-monolayer supports of rather high altervalent capacity, capable of withstanding alkaline media as well, have been selected to investigate the primary oxide and H-adatoms spillover properties. In other words, the preceding experimental evidence has unequivocally shown that the higher the altervalent capacity of the interactive hypo-d-oxide, or of the amount of mixed valence catalyst support, the more pronounced and the higher the initial positive potential values become to start the ORR,[9−11,16] step by step successively approaching the ROE features. In this respect, cyclic voltammograms scanned upon $Pt/WO_3,TiO_2/C$ ($Pt/Nb_2O_5,TiO_2/C$, and/or $Pt/Ta_2O_5,TiO_2/C$) electrocatalyst at low moisture content of He stream (just enough to enable basic electrode processes to proceed), insufficient for WO_3 (or TiO_2) hydration, (eq 1a), repeatedly reveal similar potentiodynamic spectra characteristic for indifferent carbon supported (Pt/C), or plain Pt itself (Figure 6), but with high double layer charging capacity, because of the accompanying parallel charging of Vulcan carbon particles beside the metal (Q_{DL} = 1.07 C, assessed by the method displayed by Schmidt et al.[80]

In contrast to such fairly common occurrences, a continuous supply of saturated water vapor in the He stream at higher temperature (80 °C), imposing condensation (Boudart spillover precondition[62−65]), and leading to the appearance of wet titania−tungstenia mixed altervalent oxide composite (the wetness spillover effect), as the interactive catalytic support, has been accompanied by the unusual phenomenon of a dramatic expansion of two reversible pairs of peaks of both the primary oxide and H-adatoms chemisorptive deposition and desorption (Figure 6). The latter have both been of unusually high spillover charge and discharge capacity values and for Pt−OH (UPD and OPD) shifted toward both much more negative *and far positive potential limits*, in common with Figure3a,b and discussion therein. In fact, the latter arises just as the effect of the Pt−OH equivalent dipole charging and discharging of the double layer! Namely, just as stated above, nothing else takes place in between. Every cessation in the steam supply instantaneously imposes the sudden reversible shrinkage of both such rather exaggerated pairs of peaks down to the same initial potentiodynamic shape similar to the nanostructured Pt/C voltammogram spectra themselves, but only with less pronounced (UPD and OPD) expansions in the double layer where charging or discharging extends. *Vice versa*, the renewed saturate water vapor feeding immediately leads to their sharp former primary oxide peaks and the same former charge capacities;[9−11,16] namely, the effect already noticed and scanned for formaldehyde[19] and formic acid[20] oxidation. Such an appearance without exception behaves as a typical reversible transient phenomenon by its endless altering repetition, and never appears upon the plain Pt/C electrocatalyst, both wet and/or dry, nor with small and insufficient amounts of catalytic hypo-d-oxide support.

Since the two distinctly different cyclic voltammogram shapes (Figure 6) appear only as the result of the difference in water

dx.doi.org/10.1021/jp412292w | J. Phys. Chem. C XXXX, XXX, XXX−XXX

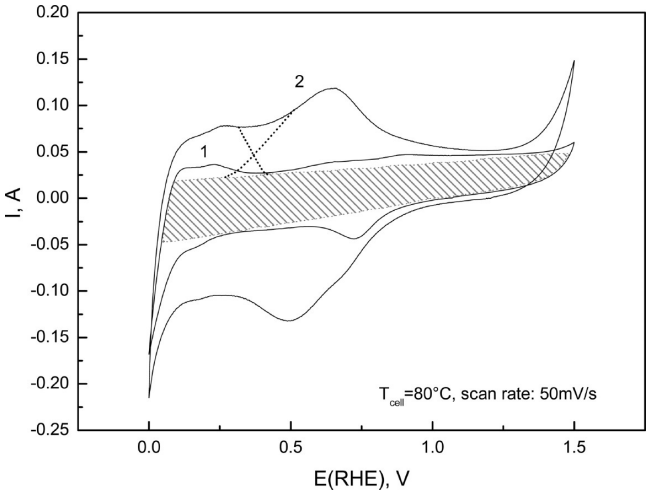

Figure 6. Cyclic voltammograms of interactive (SMSI) supported nanostructured Pt electrode ($Pt/WO_3,TiO_2/C$), on mixed valence hypo-d-oxides, scanned in He stream, at negligible moisture content (curve 1) and at 80 °C water vapor saturation (curve 2).

vapor supply, and other parameters being unaltered, an unequivocal theoretical conclusion, as well as the best heuristic experimental confirmation have been derived from the interfering interactive character and specific interexchangeable double (H-adatoms and Pt−OH) spillover properties of an unique altervalent hypo-d-oxide structure under directional electrode features of polarized nanostructured Pt electrocatalyst. The deconvoluted cyclic voltammograms clearly reveal the mutual merging of two otherwise independent spillover peaks for both Pt−H and Pt−OH adsorption and desorption, with far-reaching positive consequences in the revertible combination of altering PEMFCs and water electrolysis (WE) operation.[13−16] The same conclusion equally concerns the equivalent combinations of Nb_2O_5, TaO_2, CeO_2 (even MoO_3) with anatase titania, which at some broader ratios, when properly thermally treated, feature very high electron conductivity (above 300 S cm^{-1})[36,37] and corresponding membrane transfer capability with equal dual spillover properties (even when missing a carbon current collector).

As a consequence, the whole phenomenon in pronouncedly more wet condensation conditions and continuous water vapor supply, like typical capillary features, is further remarkably more facilitated both in the reversible cathodic H-adatoms spillover yielding Pt-bronze and/or, *vice versa*, its anodic transfer into the hydrated state and sources ($W(OH)_6$, $Ti(OH)_4$, $Nb(OH)_5$, $Ta(OH)_5$), $Ce(OH)_4$) for Pt−OH effusion, both being extremely fast reversible reactions. Thus, the primary oxide dipole species undertake both the unusually pronounced double layer charging role and/or exaggerated reversible UPD and OPD adsorption and corresponding desorption within much broader potential range and in dependence on available adsorptive Pt and active carbon surface. Consequently, the whole system behaves pronouncedly reversibly and smoothly alterpolar interchangeably both for the Pt−OH and H-adatoms spillover, and as a whole, in the reversibly revertible alterpolar coexisting equilibrium interrelation between tungsten bronze and its hydrated state ($Pt/H_{0.35}WO_3 \Leftrightarrow Pt/W(OH)_6$), as well as for all other considered congenial hypo-d-oxide altervalent combinations ($Pt/H_xNb_2O_5 \Leftrightarrow 2Pt/Nb(OH)_5$). In other words, two coexisting and mutually interfering reversible pairs of peaks fast altering between H-adatoms (adsorption or desorption) effusion and Pt−OH spillover (and/or its backward removal) along the potential axis, with all interacting consequences imprinted upon cyclic voltammetry spectra, inherently testify by their exaggerated potentiodynamic features to the reversible interrelations between two coherent dual alterpolar electrode properties. In addition, the extremely fast H-adatoms spillover within the hypo-d-oxide structure highly facilitates their effusion over carbon catalyst support.[75−78] This experimental evidence implies the equivalence in the endlessly repeatable reversible alterpolar changes and stable electrocatalytic properties of L&M PEMFC in conjunction with equally catalytically advanced WE. In this respect, both peaks of Pt−OH adsorption and desorption are equal and of enormous charge capacity ($Q_{Pt-OH(a)} = Q_{Pt-OH(c)}$ = 1.453 C), like a DC capacitance of extremely developed electrode surfaces, and since they are highly reversible and evidently behave pronounced the latent Pt−OH storage (cf. refs 21−28), they keep the same extents even after multiple and repeating number of cycles at any other time. These experimental facts imply conclusive remarks about an already known phenomenon[75−78] that the bipolar primary oxide structure establishes the reversible transient adsorption and charging capacity even on usually developed active carbon surface (C−OH), but by no means takes place in its oxidation.[8−16] The latter statement has been confirmed by an *online* mass spectrometer, which identifies CO_2 only within the oxygen-evolving potential limits. The fast spillover of H-adatoms over also reversibly fast renewing tungsten bronze ($Pt/H_{0.35}WO_3$) out of its interrelating hydrated state ($Pt/W(OH)_6$), including its own nonstoichiometric stored H-adatoms, along with adsorptive effusional deposition on, and subsequent desorptive removal from, exposed carbon surface, in such a way continuously behaves as its auxiliary storage.[75−78] The partial participation of moisture in the gas stream supply, along with the available adsorptive surface of the electrode, define the extent of the charge capacity both for the Pt−OH peak itself and DL extension and growth, a phenomenon that has never been marked on the RDE and any other polished plain Pt type electrodes in aqueous media. Even more so, now ending (or, starting) with the reversible oxygen electrode potential (1.29 V vs RHE) (Figures 6, 7 and 8). Due to the increased moisture content, now the H-adatoms UPD desorption peaks directly merge with the prevailing broad reversible primary oxide spillover deposition and appear in dramatically expanded charge capacity (247 versus 47 mC cm^{-2}, or in the ratio of about 5.3:1). In fact, 0.4 mg Pt cm^{-2} effectively corresponds to 200 cm^2 of exposed Pt surface (B.E.T. assessed 50 m^2 g^{-1} Pt), or to 42.0 mC cm^{-2} of charge capacity per projected geometric surface of electrode, in good agreement with the UPD H-adatoms-determined desorption value under dry conditions. Exactly the same relates to the H-adatoms adsorption and Pt−OH desorption peaks in the equivalence to their corresponding reversible counterparts.

The enriched potentiodynamic experimental evidence, in accordance with the instantaneous reversibly revertible alterpolar properties of the bronze-type electrocatalysts and extremely broad potential range of the primary oxide adsorption and desorption, unambiguously testify now that the Pt−OH (AuOH, M−OH) in aqueous media both UPD and OPD charges and discharges DL (eq 1), and thence is available all along for reaction within unusually wide potential limits.

Two complementary interactive Ta_2O_5-based electrocatalytic supports strongly reinforce just displayed potentiodynamic features of $Pt/WO_3,TiO_2/C$ by their coinciding and congenial spectral behavior: (i) The distinct growth of Pt−OH and H-adatoms adsorption and desorption peaks, reflecting their different accumulated latent charge capacities, as a function of the

dx.doi.org/10.1021/jp412292w | J. Phys. Chem. C XXXX, XXX, XXX−XXX

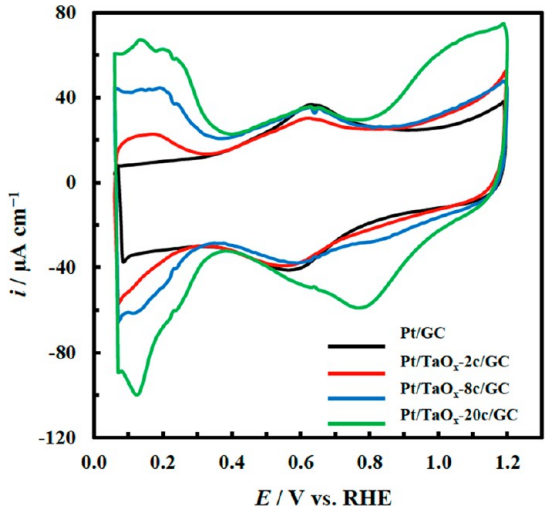

Figure 7. Cyclic voltammograms scanned at the Pt/GC and Pt/TaOx/GC catalytic electrodes with 2c, 8c, and 20c (cycles) in Ar-saturated 0.5 M H_2SO_4 solution at scan rate of 50 mV·s^{-1}, revealing the effect of proportional increasing of interactive Pt supporting Ta_2O_5 deposit on the Pt−OH spillover effect and growth for the ORR (courtesy of T. Ohsaka[22]).

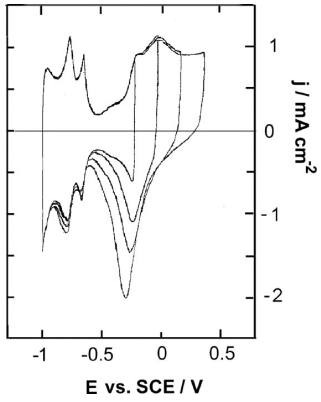

Figure 8. Potentiodynamic stepwise traversing sweeps of Pt microspheres electrodeposited on initially polished metal Ta surface, after cyclic development of its Ta_2O_5 interactive hypo-d-oxide layer support (2.3 nm), scanned in 1.0 M NaOH toward oxygen evolving limits with sweep rate of 50 mV·s^{-1} (courtesy of S. Mentus[81]).

amount (charge density) of interactive composite hypo-d-oxide deposits per unit electrode surface (Figure 7), Ohsaka et al.,[22] and (ii) Stepwise scanned voltammograms, Figure 8, revealing both continuous growth of the Pt−OH charge density (and/or its capacity) in adsorption, and corresponding desorption, mostly consisting of the reversible peaks, when in the opposite scan direction.[81] In other words, the higher the interactive hypo-d-oxide accumulative deposition[22] (or its sol−gel growth), the higher the Pt−OH latent storage in its charge capacity, and correspondingly, the more positive, and thereby the more reversible the starting potential value for the ORR becomes (Figures 6, 7 and 8). In fact, such Pt−OH latent storage growth (including the corresponding spillover effect) does not extend endlessly and usually passes over the remarkably pronounced maximum in the ORR catalytic rate and activity (see Figure 11, ref 74]).[82] At this point it should also be stressed that all three congenial cyclic voltammograms (Figures 6, 7 and 8) exhibit the reversible properties of the ROE all along the corresponding and relevant potential range, back and forth, and thence end up traversing anodic potential with evolving oxygen at the thermodynamic equilibrium value (1.29 V vs RHE), while, in all these issues, the latter occurs straight from the primary oxide peak:

$$4Pt{-}OH \leftrightarrow O_2 + 2H_2O + 4Pt + 4e^- \quad (6)$$

In other words, Pt (Au) electrocatalysts selectively and interactively grafted on hypo-d-(f)-oxide supports, in general exhibit enriched latent storage and the corresponding primary oxide spillover, so that the reversible anodic oxygen evolution (eq 6) takes place straight from pronouncedly exaggerated Pt−OH (Au−OH) adsorptive peak capacities (Figures 6 and 7) and, thence, at the thermodynamic equilibrium (ROE) potential value, while in classical issues (Figure 1b), the latter occurs from the strong irreversible deposited and highly polarizable monolayer of the Pt═O, and thereby, at rather high anodic overpotentials.

What is now the substantial difference between voltammograms in Figure 4a,b, and Figure 6 (or Figure 7) for the wet state? Even when mostly deprived from the surface oxide (Pt═O) adsorptive growth (Figure 4a,b), the reversal backward cathodic scans on plain Pt remain highly polarized for about 600 mV with negligible or zero current, exactly corresponding to Figure 1b. In other words, there is still no stored Pt−OH on plain Pt to start the self-catalytic interfering reaction (eq 3c) of the ORR, or HCHO oxidation. However, on the hypo-d-oxide interactive supported Pt catalyst, the *a priori* latently accumulated initial storage of the primary oxide from the beginning is ready and available, and thence continuously provides and spillover enhances the latter to proceed as the uninterrupted and limitless (in an exaggerated values sense) reversible electrode reaction, as long as there is continuous water vapor supply. However, for the plain Pt (or Pt/C), the sudden hysteretic sharp anodic current jump in the course of reversal cathodic sweep (Figure 4a,b) rearises at and coincides with the classical position of the reversible peak of the primary oxide growth,[2−5] reflecting the local interfering self-catalytic effect at such potential range provided by the repeated Pt−OH spillover growth. This is the striking point and the core substance of the present study.

Even more so, so far the electrocatalytic activity growth for the same unchanged exposed Pt (Au) surface has been unimaginable, but only with and as a function of the increased amount of the interactive hypo-d-oxide support (Figure 7). Meanwhile, the former is associated with and arises as the function of spillover properties, and consequently, depends on the available latent storage surface area, or the number of active centers per unit support surface.

In fact, the initial idea for the extension of reversible features in the broader potential range for the ORR, with all consequences discussed above, arose from the thorough examination of potentiodynamic growth behavior of ruthenium oxide films by Hadzi-Jordanov et al. (Figure 6 of ref 83).

PRIMARY OXIDE SPILLOVER DL CHARGING AND DISCHARGING IN LIGHT OF THE FIRST PRINCIPLE THEORY

The overall summation (Σ) for the ion exchange properties of hypo-d-oxide hydrated membrane transferring matrix, under directional electric field effect or polarization, yields reversible Pt−OH adsorptive and/or desorptive spillover upon or from a metal electrocatalyst reactive surface, resulting that way with the characteristic pronounced reversible effusion peaks of extremely fast electrode reaction,[2−5] (eqs 1a, 1b and 1c, yielding by such a summation the same former eq 1′),

dx.doi.org/10.1021/jp412292w | J. Phys. Chem. C XXXX, XXX, XXX−XXX

$$M + H_2O \leftrightarrow M - OH + H^+ + e^- \quad (1)$$

The starting first principle thermodynamic relation for such an SMSI (exampled as M/TiO_2) system and just defined general reversible peak reaction (eq 1) arises therefrom in the following form:

$$\bar{\mu}_{H^+} = -\mu_{M-OH} - \bar{\mu}_e + \mu_{H_2O} + \mu_M \quad (7)$$

while from the main general self-explanatory relation for electrochemical potential definition,

$$\bar{\mu}_e = \mu_e - e\varphi = \mu_e - e\psi - e\chi \quad (8)$$

and particularly for hydronium ion (H_3O^+, abbreviated for simplification as H^+), there from eq 8 further follows an alternative relation,

$$\bar{\mu}_{H^+} = \mu_{H^+} - e\varphi_{H^+} \quad (9)$$

To avoid and eliminate electrochemical potentials ($\bar{\mu}_{H+}, \bar{\mu}_e$), by equalizing the right-hand sides of eqs 7 and 9, and replacing the corresponding value from eq 8, it straightforwardly yields the following relation:

$$\mu_{H^+} = -\mu_{M-OH} + \mu_M + \mu_{H_2O} + e\varphi - \mu_e + e\varphi_{H^+} \quad (10)$$

Meanwhile, since $\varphi = \varphi_{H^+} + \chi = \psi + \chi$, and thereby, $\varphi_{H^+} = \psi$, it further follows,

$$\mu_{H^+} = -\mu_{M-OH} - \mu_e + \mu_M + \mu_{H_2O} + 2e\psi + e\chi \quad (11)$$

Finally, by taking the derivative of eq 10, because $\Delta\mu_e = 0$, and since μ_M, μ_{H_2O}, and ψ = const, while $\Delta\mu_{H^+} \ll e\Delta\chi$, it straightforwardly results,

$$\Delta\mu_{(M-OH)} = e\Delta\chi \quad (12)$$

exactly as cyclic voltammograms (Figure 6) reveal: Every change in spillover of the M−OH, or of its chemical potential ($\Delta\mu_{M-OH}$), as the driving force of the effusion, or, simply its concentration variations, corresponds to the increment of surface potential ($\Delta\chi$), or the change in capacity of DL because of the M−OH dipole adsorption package, or desorption (as the spillover capacity), both of them being fast and substantially reversible, define DL charging or discharging (in its capacity). Namely, since $\Delta\mu_{H^+}$ is a logarithmic function of hydronium ions concentration, and according to the spillover electrode reaction (eq 1), primary oxide (M−OH) and H_3O^+ ions become simultaneously spent or produced in equivalent (1:1) amounts, while the contribution of surface energy is the linear function of surface potential (prevailing dipole effect), $e\Delta\chi$, then the inequality conclusion, $\Delta\mu_{H^+} \ll e\Delta\chi$, emerges quite logically.

Since the fundamental definition of work function (Φ) states[84,85] that

$$e\Phi = -\mu_e + e\chi \quad (13)$$

and taking into account eq 12, by derivation of the latter (eq 13), there straightforward follows the broader fundamental definition for M−OH spillover adsorption and/or desorption, which is the same as the DL capacitance charging and/or discharging,

$$e\Delta\Phi = e\Delta\chi = \Delta\mu_{M-OH} \quad (14)$$

Simple combination of eq 13 with eq 8, then yields the alternative first principle relation between work function and electrochemical potential,

$$\bar{\mu}_e = -e\Phi - e\psi \quad (15)$$

which, for the considered issue of electrochemical cell (U_{WR}), assembled between working (W) and stable reference (R) electrode, can be straightforwardly written to read,

$$\Delta\bar{\mu}_e = \Delta U_{WR} = -e\Delta\Phi - e\Delta\psi \quad (16)$$

The main contribution to both changes in work function ($\Delta\Phi$) and primary oxide dipole spillover ($\Delta\mu_{M-OH}$), comes from the surface potential increment ($\Delta\chi$) itself (eq 12), as the prevailing part of inner or Galvani potential ($\Delta\varphi$). Namely, Vayenas et al.[86,87] have proved on plentiful systems in solid state electrolyte,[88] aqueous media,[89−91] and PEM Nafion 112[92] the basic NEMCA or EPOC promotion relation in heterogeneous catalysis,

$$\Delta U_{WR} = e\Delta\Phi \quad (17)$$

that could also be considered as fundamental in both electrode kinetics[93−95] and spillover phenomena.[96] Meanwhile, the latter (eq 17), when correlated with the preceding relation (eq 16), unambiguously and consequently yields

$$\Delta\psi = 0 \quad \text{or} \quad \psi_W = \psi_R = \text{const} \quad (18)$$

which is also implied in above preceding equations (eqs 11 and 12).[97,98] Such a conclusive and far-reaching statement is in particular reliably clear for the electrode steady state and with high concentration supporting electrolyte.

The whole thermodynamic equilibrium for the general issue of interactive (SMSI) metal/hypo-d-oxide supported catalyst, such as M/TiO_2, is now illustratively displayed in all interconnected energy details by Figure 11 in ref 8. As a consequence, any decrease of the M−OH chemical potential ($\Delta\mu_{M-OH}$), causes the work function to decrease correspondingly, and *vice versa*. In other words, any consumption of adsorbed M−OH upon metallic catalyst surface causes its chemical potential to decrease, and this way imposes imbalance within the established equilibrium. Thus, to keep constant both $\Delta\Phi$ and cell voltage between working (W) and reference (R) electrode (ΔU_{WR}), the titania phase, by its enriched latent storage of the primary oxide, automatically reacts by its membrane transferring mechanism and supplies hydroxide ions (Scheme 1), to emanate further as the primary oxide spillover adsorptive species on exposed metallic catalyst surface by corresponding electrocatalytic reaction (eq 1), both from hydrated anatase structure and by reacting of continuously supplied water molecules.

The overall conclusion associated with otherwise broad experience in electrochemical promotion (NEMCA, EPOC)[84,86,87] of various chemical reactions in heterogeneous catalysis and particularly for Doebereiner (Ertl interpretation[17]) oxidation of hydrogen in water solutions, for catalysts interactive (SMSI) supported upon hypo-d-oxides, OH^- ions play the main membrane transferring and decisive promotion role, while M−OH, as the defined dipole state, undertakes the spillover and features as the substantially reacting species all over the metallic catalyst surface, enabling a way to keep such thermodynamic equilibrium established. In fact, there is no catalytic promotion for hydrogen oxidation in acidic aqueous media, and apparently hydroxide ions impose such a substantial promoting efficiency, in particular within the interfering (600−900 mV vs RHE) potential range, when NEMCA approaches promotion effects of 2 orders of magnitude.[88,89] Therefore, any disturbance of such an equilibrium, such as the consumption of spillover adsorbed M−OH species ($\Delta\mu_{M-OH}$), or simple imposition of an external polarization, as just analytically shown above, reflects as the

dx.doi.org/10.1021/jp412292w | J. Phys. Chem. C XXXX, XXX, XXX−XXX

driving force ($\Delta U_{WR} = e\Delta\Phi$), and instantaneously tends to reestablish the former equilibrium, or to keep its steady state.

Since the adsorption of the primary (M−OH) oxide plays a decisive and critical role in many important (electro)catalytic processes, in particular for CO tolerance and the ORR, enthalpies of chemisorption might throw some light for *a priori* considerations and estimative assessments. Namely, from the measured isosteric heat of Pt−OH adsorption (ca. 200 kJ/mol), the adsorptive Pt(111)−OH bond energy was estimated to be ca. 136 kJ/mol, that is, much less than the surface (Pt═O) oxide chemisorptive bonding energy (ca. 350 kJ/mol), and this is taken as the argument for higher catalytic activity of the former in surface electrochemistry of CO.[99] In fact, a rough estimation of adsorptive energy for interactive supported Pt catalysts upon hypo-d-oxides tells that the above ratio might even be for an order higher, and consequently Pt−OH correspondingly more active in heterogeneous catalysis and particularly for the ORR. Otherwise, since two Pt-oxides, Pt−OH and Pt═O, distinctly differ in their polarization of desorption and/or adsorption, and since the latter defines the enthalpy of adsorption, such pronounced overvoltage differences unavoidably should have to imply their corresponding adsorptive/desorptive enthalpy values and differences. In the same context, hydrogen atoms from bronze-type interactive supported Pt electrocatalysts (Pt/$H_{0.3}WO_3$) are distinctly more electrocatalytically and catalytically active than H-adatoms from plain nanostructured (Pt/C), and feature much weaker adsorptive bonding strength.

INTERFERING M−OH VS M═O SPILLOVER SYNERGISM AND ELECTROCATALYTIC POTENTIAL SHIFT FOR THE REVERSIBLE ORR

The same congenial conclusive remarks and observations yielding from the striping voltammetry CO tolerance, XPS, EELS, EDXS, FTIR, DRIFT, and potentiodynamic spectra analysis[8−16] have clearly been that the anodic Pt−OH spillover effect and its contributions are unequivocally manifold confirmed by these mutually straightforward correlating experimental methods and corresponding experimental evidence, and smoothly proceed with high catalytic rates. However, cathodic ORR mostly starts with already completed Pt electrocatalyst Pt═O coverage ($\Theta(Pt{=}O) \rightarrow 1$), and thereby imposes rather high reverse polarization ($\eta_c \geq 600$ mV, Figure 1a,b), where the interfering Pt−OH spillover faces an unusually high energetic activation barrier to overcome and provide the corresponding catalytic effect. In other words, cyclic voltammetry spectra clearly reveal the Pt═O desorption (eq 2), as the main polarization impact within the whole ORR mechanism. Thus, to enable the break across the strongly adhering adsorptive Pt═O layer, new interactive (SMSI) electrocatalyst supports imply the mixed valence hypo-d-, and recently even mutually composite hypo-f-oxide supports of unusually high latent Pt−OH storage,[10−16,21−28] establishing multiple interfering equilibrium of various strengths in the hydroxide membrane type transfer (eqs 1a, 1b, and 1c), resulting in the Pt−OH release and spillover spreading even in the initial course of otherwise the highest value cathodic polarization. In other words, cathodic spillover of the Pt−OH and other primary oxides is extremely fast, and each (eq 1′) for its own independent electrode process (Figures 6, 7 and 8), as well as their reactions upon the electrocatalytic surface. Thus, only the multiple and enriched interactive hypo-d- and in particular mixed and composite hypo-f-oxide supports, enable enough interfering shift of the initial reversible ORR potential closer to, and even approaching now already confirmed the ROE potential value. In such a respect, the best so far obtained interactive composite hypo-d-f-oxide support structures being Pt/Nb_2O_5,TiO_2,CeO_2/C, Pt/Ta_2O_5,TiO_2,CeO_2/C, and Pt/Nb_2O_5,Ta_2O_5,TiO_2,CeO_2/C. Such state of composite electrocatalysts enables us to now deal with and substantiate the reversible ORR electrode in L&MT PEMFCs and dramatically increase the efficiency in the energy chart diagram (Figure 1a). The point and substance consist in proper mixed valence compounds of various altervalent capacity hypo-d- and hypo-f-oxides to provide remarkably increased latent storage and then intensified generating spillover of primary oxides. At the same time, this implies increased number and values of interrelating multiple equilibria characterizing the membrane transfer within the composite (network) matrix, enabling the permanent presence of primary oxide(s) in the course of the fast cathodic reaction, finally resulting in the interfering synergistically facilitated reaction with the Pt═O (eq 3c), and thereby the substantially interferential shift of the positive limits of the starting electrode potential for the ORR.[10−16,21−28,34−45]

Primary oxides represent the adsorbing species of anodic polarization and the subject of extremely fast independent reversible desorbing items in the cathodic reaction (eq 1′), so that any adsorptive accumulation ($\Theta(M{-}OH) \rightarrow 1$) in the course of ORR is (absolutely) inconsistent, and thereby impossible, except at remarkably lower reaction rates, as the small reactive steady state amount: The faster the reaction rate, the smaller the latter ($\Theta(M{-}OH) \rightarrow 0$), or the latter results as the latent accumulation within enriched amounts of deposits of the interactive hypo-d-f-oxide supports. Meanwhile, the entire cathodic ORR mechanism implies some fast consecutive reaction steps including the Pt−OH participation, (eqs 3a,3b, and 3c), and thereby, one more substantial reason for the absence of any adsorptive surface accumulation of the M−OH in the course of cathodic polarization. In such a respect, one of the fastest reaction steps in the whole ORR mechanism, certainly represents the interfering of the Pt−OH spillover interplay with the Pt═O (eq 3c), which is the striking substance in the ORR kinetics. Meanwhile, such state of the art thence testifies that one of the decisive and conclusive axioms would now be that any reacting species could by no means at the same time be both the participant of fast steps and the rate determining species in the lowest RDS. The substantial and decisive point is that virtually Pt/C and Pt/Nb_2O_5,TiO_2/C are by no means the same things in kinetics and (electro)catalysis of the ORR!

In general, as the conclusive remark, the point and substance are that hydrogen molecules undergo spontaneous and straight catalytic dissociative adsorption upon Pt surface, and then feature fast spillover of H-adatoms over nanostructured Pt-bronze.[62−65] On the contrary, since oxygen misses such reversible adsorption and desorption properties, and it inevitably irreversibly grows as the stable Pt═O, to establish and continuously keep uninterrupted reversible features of ROE, we need such a strong interactive and selective graft bonding hypo-d-oxide support (SMSI), providing the enriched latent storage of Pt−OH. In other words, there is no ROE without the reversible spillover and adsorption of Pt−OH on the exposed Pt electrode surface and the established corresponding thermodynamic equilibrium ($Pt(O_2)/(Pt{-}OH,Pt{=}O/OH^-)$). This means that, while thermodynamically defined and *a priori* predicted dissociative adsorption and spillover of H-adatoms are spontaneous occurrences on Pt, Pt═O chemisorption is an irreversible strongly bonded, highly polarizable surface deposit and requires (SMSI) optimal mixed valence hypo-d-(f-)oxide compounds and its

dx.doi.org/10.1021/jp412292w | J. Phys. Chem. C XXXX, XXX, XXX−XXX

latent storage of Pt−OH to impose (this way spontaneously induced) the fast reversible effusion from the initial stage of the reaction, enabling Pt to behave as the ROE all along the potential axis between hydrogen and oxygen evolving limits. In such a context, from every cyclic voltammogram is visible (Figures 6, 7, and 8) the oxygen evolution straight at its reversible (1.29 V vs RHE) potential and directly from the Pt−OH species, and thence, *vice versa,* starting the ORR from the same value and with the same species.

The main point and conclusion of substantial significance are that, as compared with all diffusion and mass transfer limited electrode processes, the primary oxide spillover enabled and occurring electrocatalytic reactions, when their densely deposited hypo-d-oxide storage catalytic supports are wet and continuously moisture supplied, absolutely look and behave as unlimited, and thence, one experiences this way provided the reversible properties of the ROE. This is why spillover processes display substantially significant, decisive, and unique features and importance in heterogeneous catalysis and electrocatalysis. In essence, this is the meaning of spillover properties in the latter. The present target for the time being has been up to 60 mV/dec Tafel slope all along to 1.0 A/sq·cm current density and overvoltage of about 0.180 V at such upper reaction rate.

HYPO-HYPER-D-D-INTERELECTRONIC BONDING AND INTERFERING SPILLOVER NATURE OF ELECTROCATALYSIS FOR HYDROGEN AND OXYGEN ELECTRODE REACTIONS

Where then lies the link between the hypo-hyper-d-d-interelectronic bonding and SMSI synergistic electrocatalytic effects in the broader interfering spillover sense? The whole electrocatalytic theory[74,100] relies on the Brewer[73] intermetallic bonding model and Friedel[101] hypo-hyper-d-d-electronic correlations. They both infer that the stronger the hypo-hyper-d-d-intermetallic cohesive bonding, the more strengthened and exposed the d-orbitals become within the ideal symmetric intermetallic phases, like $ZrNi_3$, $HfPd_3$, $MoPt_3$, $LaNi_5$, $La_xCe_{(1-x)}Ni_5$, etc., and thereby the weaker and easier the cleavage of their adsorptive intermediates (Pt−H) in the RDS, and consequently, the higher the reaction rate and the overall catalytic activity.[8−16,74,100] The same Brewer[73] type d-d-intermetallic bonding model has been previously anticipated as the basis for the Tauster[69−72] promotional SMSI effect, with the far-reaching consequences in both heterogeneous catalysis and electrocatalysis. The latter systematically predetermined interactive grafting,[8,9,14,15] and the homogeneous, even uniform distribution of individual and prevailing hyper-D-metallic catalysts upon hypo-d-oxide supports.[10−13,16] The same type of hypo-hyper-d-d-interactive bonding between nanostructured metal particles of such composite catalysts and their hypo-d-oxide supports additionally reinforces the entire electrocatalytic activity effect based on the overall interactive d-d-interelectronic bonding strength, similarly as cohesive energy itself defines and advances the electrocatalytic activity for nanostructured monophase systems.[100] In fact, the interactive hypo-hyper-d-d-interelectronic bonding strengths belong to the strongest bonding effectiveness in all of chemical science,[9] sometimes even proceeding so vigorously with exceptionally intense explosion ($HfPd_3$), and thereby resulting in extra high intermetallic phase stability,[73] and consequently high electrocatalytic activity for the HER.[100] The pronounced cathodic and anodic yielding interactive spillover contributions within and based on the SMSI have been significant for the present theory and its embodiment in electrocatalysis of hydrogen and oxygen electrode reactions for L&MT PEMFC and WE.[8−16] While in aqueous media, plain nanostructured Pt (Pt/C) features the catalytic surface properties of Pt−H and Pt═O, missing any effusion of other interacting species, a new generation of composite interactive supported (SMSI) electrocatalysts in condensed wet state primarily characterizes extremely fast reversible spillover interplay of either H-adatoms, or the primary oxides (Pt−OH, Au−OH), as the significant pronounced synergistic advanced interactive electrocatalytic ingredients.[8−16]

Volcano plots of various physical and chemical properties along transition series reveal the periodicity features of elements,[102,103] based on the d-d-electronic correlations,[101] with similar symmetric shape, and consequently, when plotted one into the other, together yield various linear interdependences like cohesive and surface free energy.[103,104] As a consequence, the d-band of transition elements has been confirmed to play a crucial role in the bonding, adsorptive, catalytic and electrocatalytic properties, and consequently, any search for advances and synergism among the latter, should be based on the d-d-interelectronic correlations and modifications.[14,15,100] Such a state of theoretical knowledge and experimental evidence leads to the conclusion that every hypo-hyper-d-d-interelectronic phase diagram behaves as a part of the Periodic Table between the two initial periods of the interacting ingredients.[103−107] Their intermetallic phases are of the same average d-electronic configuration replacing the missing elements in their energy state and behavior in between and, consequently, have been used to assess the synergistically active electrocatalysts for the HER (Figure 1, ref 10). These theoretical and experimental facts can then be employed to assess the synergistically active electrocatalysts from the peak values of corresponding volcano plots along each hypo-hyper-d-d-interelectronic phase diagram,[103,105] and further catalytically advance by the interactive hypo-d-oxide interfering spillover contribution,[8−16] displayed more systematically and more thoroughly in the present study. Thus, one of the guiding aims should to be to assess experimentally or theoretically, and consequently correlate the actual hypo-hyper-d-d-interelectronic SMSI effect or hypo-hyper-d-d-interbonding effectiveness for new type interactive supported composite (Pt/Nb_2O_5,TiO_2/C, Pt/Ta_2O_5,TiO_2/C, or more complex composites for the HER, $HfPd_3/Nb_2O_5$,TiO_2/C) electrocatalysts. The formal difference is that interactive bonding is interatomic or intermetallic (Brewer−Friedel correlations), while in the more complex Tauster SMSI sense,[69,72] they are interionic-intermetallic interactions, or all together being hypo-hyper-d-d-interelectronic bonding correlations in electrocatalysis.

SIGNIFICANCE AND EXPERIMENTAL EVIDENCE FOR THE SMSI D-D-EFFECT

In such a context, to study, gain some insight in, and assess experimentally the SMSI bonding effect itself and further impose its resulting spillover phenomena, very fine, nanosized Au films were deposited by controlled electron beam evaporation of ultrahigh-purity gold metal under high vacuum onto stationary, nanocrystalline anatase titania-coated microscopic slides.[10,11] The XP spectra of the Au 4*f* electrons reveal the remarkable binding energy shift (Figure 9) that provides the insight for the d-d-interelectronic SMSI within the Au/TiO_2 interphase, and this has been one of the first experimental evidence of that kind in heterogeneous catalysis. The smaller the nanoparticle size or the thickness of the Au nanolayer, the larger the binding energy shift

dx.doi.org/10.1021/jp412292w | J. Phys. Chem. C XXXX, XXX, XXX−XXX

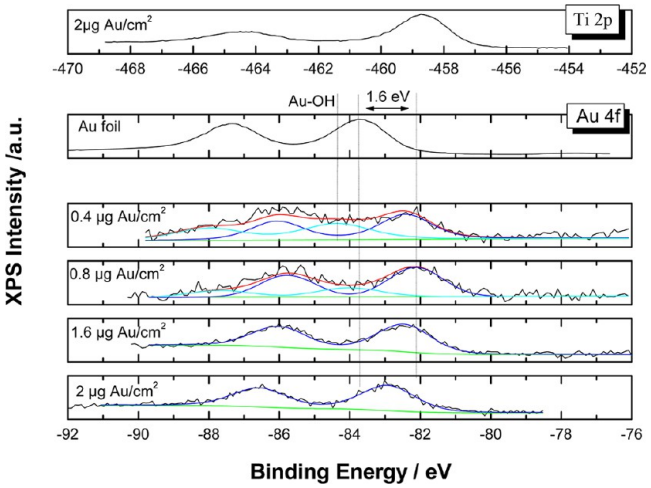

Figure 9. XP spectra of Au 4*f* for vapor deposited nano-layered Au upon a fine thin film of anatase titania with deconvolution for lower amounts of deposits to reveal the existence of primary oxides (Au−OH and AuOOH) and the corresponding (Au/TiO_2) hypo-hyper-d-d-binding (SMSI) energy.[11]

in the XP spectra with titania, and the more pronounced the d-d-SMSI effect, with tendency to its maximal d-d-binding strength at monatomic dispersion (as extrapolated straight assessed value), and for 1:1 deposition of Au on available Ti atoms, as theoretically predicted in the present and preceding papers.[8−16,79] Due to the nanodimensions of the Au layer, the signal originated mainly from Au/TiO_2 interface, reflects the bonding status within the latter. In other words, the thinner the nanolayer, the closer to the interphase itself (Au/TiO_2) penetrate spectral beams and thereby, better and more completely reflect the bonding status within the latter, this way enabling one to gain some insight and feeling as concerns the hypo-hyper-d-d-interelectronic SMSI bonding effect, which is apparently very strong.

The deconvoluted Au 4*f* peaks with lower Au loadings reveal that Au nanoparticles in interactive bonding contact with titania appear partially oxidized.[108,109] The peak located at 82.15 ± 0.1 eV is attributed to metallic Au, while the peak at 84.05 ± 0.1 eV corresponds to the gold primary (Au−OH or AuOOH) oxides. The latter, in accordance with the present theory, appear as the *a priori* naturally provided primary oxide spillover species, associated with and promoted by the wet anatase titania interaction (eq 1), and are in advance, already available and ready for the cathodic ORR and anodic CO, aldehyde group and other oxidation processes.

Starting with their plain combinations (Au/C versus Pt/C) of nanostructured electrocatalysts, and in particular with interactive SMSI-supported bronze-type ($Au/Nb_2O_5,TiO_2/C$ versus $Pt/Nb_2O_5,TiO_2/C$) issues, Au is definitely a much better and advanced nanosized catalytic material for the ORR than Pt, primarily because of the remarkably smaller adsorptive strength of corresponding spillover Au−OH versus Pt−OH reacting species.[110]

Haruta et al.[111−113] have, for example, in such a sense shown that the same reactants (propylene in admixture with equimolar amounts of hydrogen and oxygen) yield different products upon different nanosized Au catalysts supported on anatase titania (Au/TiO_2): (i) Propane by hydrogenation at nanoparticles <2 nm Au, and (ii) Propylene oxide by epoxidation or oxygen addition for >2 nm Au. Hydrogenation implies H-adatoms adsorption on Au that should not spontaneously occur on a pure massive bulky gold surface. Haruta[114−117] ascribes such chemisorptive properties to "forced" or strained Au-d-orbitals within smaller (below the critical threshold) nanostructured metal particles, in particular when d-d-SMSI deposited on the interactive anatase titania (cf. 11,100). In other words, smaller nanostructured Au particles (<2 nm), interactively d-d-bonded with anatase titania, or in particular when interactively supported upon mixed valence hypo-d-d-compounds ($Au/Nb_2O_5,TiO_2$, $Au/Ta_2O_5,TiO_2$, or $Au/WO_3,TiO_2$), thereby being even more reinforced in their d-d-interbonding effectiveness, and thence exposed with the more strained d-orbitals, are qualitatively different than massive Au. Such highly dispersed nanoparticles consequently exhibit H-adatoms adsorption, and this feature provided the reversible behavior of the hydrogen electrode in the Nernst sense,[11] and finally, is thereby able to carry out the hydrogenation processes, a property so far unknown for gold at all. Such defined smaller (<2 nm) Au nanostructure is something else both in heterogeneous catalysis and particularly electrocatalysis, than massive Au ("the most noble and most inactive noble metal"),[110,118] primarily because of featuring spontaneous H-adatoms adsorption.[11,100] In the same context, it has been further shown that a self-reconstructed Au electrode surface, after multiple potentiodynamic cycles between hydrogen and oxygen evolving limits, features the pronounced H-adatoms adsorption and even absorption, and consequently, the reversible electrode properties (M. M. Jaksic et al.,[11] and references therein). The reconstruction effect has been much more pronounced and faster in heavy water media, because of the stronger interatomic interrelations and deeper penetrating interphase effect of twice larger deuterium than protium ions and atoms.[11] Finally, the advanced electrocatalytic properties of sol−gel prepared nanostructured Au for the HER, and extra superior for the ROE, and even Ag (Ag, $AgNi_3$, $AgNiCo_2$) for alkaline media, after homogeneous interactive SMSI grafting deposition upon carefully supercritical dried hypo-d- and hypo-d-f- mixed valence compounds in liquid CO_2, ($Au/Nb_2O_5,TiO_2/C$, or $Au/Ta_2O_5,TiO_2,CeO_2/C$), follow in the forthcoming studies.

NANOSTRUCTURED CHARACTERIZATION OF HYPO-D-OXIDE SUPPORTED ELECTROCATALYSTS

The correlation of XRD spectra and ultrahigh-resolution transmission electron microscopy (UHRTEM) and in particular scanning transmission electron microscopy in high-angle annular dark field (STEM-HAADF) mode (also known as Z-contrast) images belongs to the most reliable methods to estimate the nanostructured particle size distribution of Pt electrocatalysts upon interactive hypo-d-oxide catalytic supports, and represents substantially the most significant nanosize analysis manner for the time being now. The spectrum for the $Pt/(Nb_2O_5,TiO_2)/C$ catalyst reveals an overlapping region between 35 and 50 degrees (Figure 10). In this region one expects the reflection lines for the Pt (111) and (200), TiO_2 anatase (004) and (200), as well as the graphite (100) crystallographic planes, indicated by the labeling straight lines drawn therein. Evidently, all the above-mentioned reflections are essentially overlapping. In this respect, it is not possible to estimate exactly the Pt and TiO_2 particles size, while peaks attributable to Nb specimens are at the noise level and absent, due to their very small amount. Nb oxide reflection peaks are also absent even from the XRD spectrum of the enriched $Pt/Nb_2O_5/C$ catalyst, although the amount of niobia is now significantly higher as compared with the $Pt/(Nb_2O_5,TiO_2)/C$ sample. The only visible reflection peak in the $Pt/Nb_2O_5/C$

dx.doi.org/10.1021/jp412292w | J. Phys. Chem. C XXXX, XXX, XXX−XXX

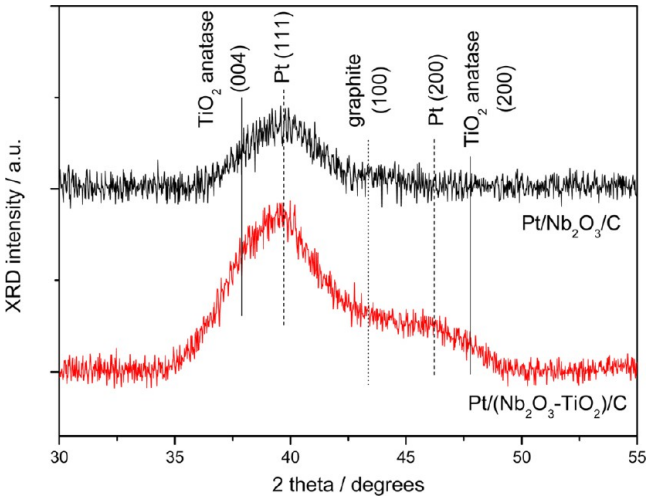

Figure 10. XRD spectra of the interactive supported Pt electrocatalysts on Nb_2O_5/C and (Nb_2O_5,TiO_2)/C. The vertical lines drawn show the positions of the respective peak reflections.

sample is ascribed to the Pt (111) crystallographic plane. By fitting this particular peak with a Gaussian function, it is possible to estimate the average Pt particle size by applying the Scherrer equation. It was found to be approximately 2.2 nm, indicating the highly and uniformly dispersed nature of such a catalyst. From hydrogen gas chemisorption measurements,[12] the average Pt particle size was estimated to be 3.7 nm (77 m^2/g of Pt assuming spherical particles, while the electrochemically active surface area, UPD H-adatoms estimated by the corresponding potentiodynamic desorption peaks, is assessed to be even lower, 57.5 m^2/g Pt). The significantly larger Pt particles are overestimated by the B.E.T. H_2 chemisorption indicates the interaction between the Pt particles and the oxide support (SMSI) that hinders the hydrogen gas adsorptive properties of Pt crystallites, leading to particle size overestimation. On the other hand, the particle size determination by XRD is usually overestimated (the overlapping effect), and since the size is close to the instrument limits, such a state of experimental evidence convincingly suggests that Pt particles are evenly dispersed and strongly bonded on the hypo-d-oxide catalytic support as shown by many XRD measurements with similar interactive hypo-d-oxide supported electrocatalysts.[8−16] The absence of niobia reflection peaks indicates that Nb-oxides are either highly sub- up to monolayer dispersed on the carbon particles surface (as essentially the surface species), or less probably in the amorphous state. In fact, the present electrocatalyst has been *a priori* planned and calculated by the mass and surface ratio between hypo-d-oxide and Vulcan carbon particles to be deposited as a submonolayer (Nb_2O_5 having 170 m^2/g, while carbon particles are in higher amount and of much larger surface area, 260 m^2/g). Such a unique XRD experimental insight convincingly testifies to the existence of high Pt (111) bronze dispersion upon highly developed hypo-d-oxide support. Such a state relative to the standard Pt/C electrocatalyst, otherwise suffering from Pt surface diffusion and agglomeration, characterizes remarkably increased electrocatalytic activity, a much longer lasting catalyst because of the SMSI bonding effect, while the interactive structure enables Pt metal recovery, which is another high-quality achievement of the novel nanostructured bronze type electrocatalysts. Meanwhile, the most significant is the control of homogeneous dispersion of grafted nanostructured Pt size magnitude: The ratio of available exposed hypo-d-oxide surface relative to the Pt 10 wt % defines the latter, and in our issues it is usually fixed between 2.0 and 2.4 nm on average, in particular for NbO_x, WO_x, and TiO_2 individual and mixed valence composite hypo-d-oxide supports (SMSI); for TaO_x, it is not yet optimized. However, TEM identifies an abundance of about 1.0 nm Pt/TaO_x/C clusters.

UHRTEM, and in particular STEM imaging in HAADF mode with aberration correction (FEI Titan 80-300), reveal grafted Pt nanoclusters on hybrid hypo-d-oxides supports, with a rather uniform and evenly homogeneous distribution on average of about 2 to 2.4 nm in size on the best issues {Pt (10 wt %)/20 wt % Nb_2O_5,TiO_2/C}, Figure 11b, {Pt (10 wt %)/20 wt % Nb_2O_5/C}, Figure 11a, and {Pt (10 wt %)/20 wt % WO_3,TiO_2/C}, Figure 11d, obtained so far and in excellent agreement with size measurement with XRD. Even more so, with three times larger Pt amount {Pt (30 wt %)/20 wt % Nb_2O_5,TiO_2/C}, Figure 11c, the homogeneous nanostructured Pt distribution keeps the same trend and in particular the average nanosize. Such a homogeneous, unusually narrow nanosize level of distribution has never so far been achieved (the interactive SMSI effect) and confirms the reliable basis for the rather pronounced spillover effect and the unique electrocatalytic achievements. No single Pt nanostructured cluster has been noticed on the prevailing carbon nanoparticles percentage of their otherwise highly developed exposed surface area, no surface diffusion, and no agglomeration, either. It would certainly be worth noticing the rather allover homogeneous widespreading of the interactive hypo-d-oxide support structure and very distinct inter-d-d-bonded and interactive (SMSI) grafted fine Pt nanosized clusters upon them, as a unique nanostructured Pt-bronze substantiation of advanced electrocatalytic properties, primarily and mostly extended by the pronounced interfering Pt−OH spillover effect for the cathodic ORR.

In addition, atomic-resolved HAADF-STEM observations strongly support the interacting (SMSI) and interfering spillover theory. The selective interactive hypo-hyper-d-d-interelectronic grafting distribution between Pt and Ta_2O_5 on the carbon support results in the interdependent Ta oxide network structure, symmetrically surrounding Pt cluster (Figure 12). High-resolution HAADF images obtained with aberration-correctors of the electron probe (0.07 nm resolution) even resolve the individual Ta atoms of the oxide network supported on the carbon (Figure 12b,c). This structure of Pt surrounded by the Ta oxide network would result, right at the interface Pt/Ta_2O_5, in the reinforcement of the overall SMSI effect at such a site, possibly with the $TaPt_3$ phase, already XPS confirmed for $TiPt_3$ (Figure 3, ref 11), and provide the highest electrocatalytic activity as the result (cf. Figure 10).

The reinforced (SMSI) hypo-hyper-d-d-interelectronic bonded nanostructured synergistic electrocatalytic composite Pt/$TiPt_3$/TiO_2 has already been approved and tested, while symmetric monatomic Ta distribution around a Pt nanocluster is the first step toward the interbonding and reinforcing $TaPt_3$ interphase at the interface Pt/Ta_2O_5, promising further electrocatalytic SMSI advances.

SUPERIOR BRONZE-TYPE ELECTROCATALYSTS FOR REVERSIBLE ALTERPOLAR INTERCHANGES IN THE REVERTIBLE (PEMFC VS WE) CELL ASSEMBLY

The striking target issue of the present paper has been to show the development and substantiation of corresponding spillover electrocatalysts for the superior revertible cell assembly for spontaneous reversible alterpolar interchanges between PEMFC

dx.doi.org/10.1021/jp412292w | J. Phys. Chem. C XXXX, XXX, XXX−XXX

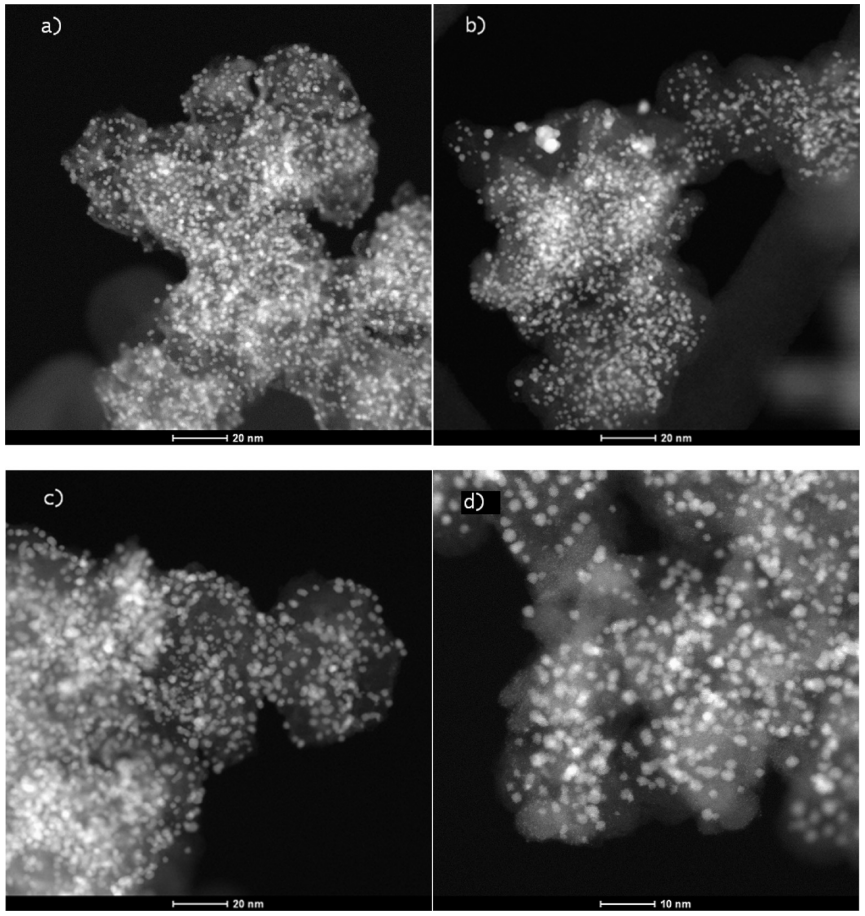

Figure 11. Scanning transmission electron microscopy images in high-angle annular dark-field mode (HAADF-STEM) of TM hypo-d-oxide/carbon support material and nanostructured Pt electrocatalyst nanoparticles. (a) Composite simple basic Nb-oxide interactive (SMSI) supported electrocatalyst, {Pt (10 wt %)/20 wt % Nb2O5/C}. (b) Congenial mixed altervalent supported electrocatalyst, {Pt (10 wt %)/20 wt % Nb2O5,TiO2/C}. (c) Composite interactive (SMSI) altervalent supported electrocatalyst of the same hypo-d-oxide structure as in panel b, but of triple higher Pt weight percentage, {Pt (30 wt %)/20 wt % Nb2O5,TiO2/C}. (d) Congenial altervalent supported electrocatalyst based on mixed W-oxide and anatase titania interactive supported Pt clusters.

and WE. In other words, L&MT PEMFCs, particularly large stationary systems, are unimaginable without revertible abilities with WE alternation, enabling one to produce hydrogen during (usually overnight) excesses in electrical energy supply, and *vice versa*, to use stored amounts of the latter as a fuel in PEMFCs, in the course of (daily) deficiencies in electricity. In aqueous media, classical plain Pt/C electrocatalysts feature catalytic surface properties of Pt−H and/or Pt═O, without any effusion of other interacting species, and such situation prevents reversible alterpolar interchanges, otherwise indispensable for the smooth revertible PEMFC versus WE systems, when both alternatives are mutually equivalent and operate in their common overall harmony. In such a respect, the present paper introduces electron conductive and d-d-interactive individual and composite (mixed valence) hypo-d-oxide compounds of increased altervalent capacity, or their suboxides (Magneli phases), as the interactive catalytic supports and therefrom provides (i) the SMSI interelectron-d-d-bonding and correspondingly improved catalytic effects, and (ii) dynamic spillover interactive transfer of the M−OH, and alternatively the free fast effusion of H-adatoms for further electrode reactions, and thereby advance the overall electrocatalytic and alterpolar activities. Since hypo-d-oxides feature the exchange membrane properties, the higher the altervalent capacity, the higher the spillover effect. In fact, altervalent hypo-d-oxides impose spontaneous dissociative adsorption of water molecules and then spontaneously pronounced membrane spillover transferring properties instantaneously, resulting in corresponding bronze-type (Pt/H_xWO_3) under cathodic, and/or its hydrated state ($Pt/W(OH)_6$), responsible for Pt−OH effusion, under anodic polarization, this way establishing instantaneous reversibly revertible alterpolar bronze features ($Pt/H_{0.35}WO_3 \leftrightarrow Pt/W(OH)_6$), as the thermodynamic equilibrium, and thereby substantially advanced electrocatalytic properties of these composite interactive electrocatalysts. Due to the dual spillover alterpolar interchanges, all four electrode reactions in aqueous media are reversibly altered (HER − cathodic hydrogen evolution; HOR − anodic hydrogen oxidation; ORR − cathodic oxygen reduction; OER − anodic oxygen evolution). In other words, the HER and OER are entirely equivalent in the operational sense to the couple of ORR and HOR, and in the revertible alterpolar interchanges between PEMFCs and WE that plain Pt by no means could enable itself, and this is the reason why we consider such an electrocatalytic system superior, and even ideal and unique. Such nanostructured type electrocatalysts, even of mixed valence hypo-d-oxide structures ($Pt/H_{0.35}WO_3$,TiO_2/C, or Pt/H_xNbO_3,TiO_2/C), have for the first time been synthesized by the sol−gel methods, including the supercritical drying with liquid CO_2, and shown to feature extra high stability, electron conductivity, and non-exchanged initial pure monobronze spillover and catalytic

dx.doi.org/10.1021/jp412292w | J. Phys. Chem. C XXXX, XXX, XXX−XXX

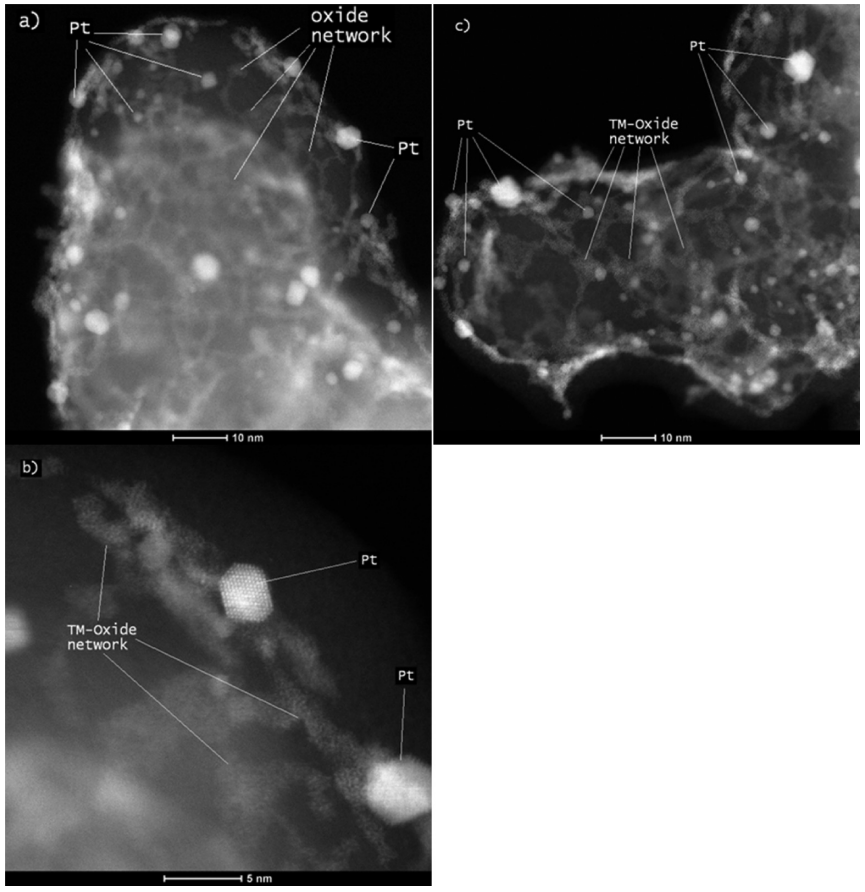

Figure 12. Atomic-resolved HAADF STEM images analysis taken in different areas of the sample. Pt catalyst particles and transition metal Ta-oxide network are identified by labels and pointed out by relevant lines in images. (a) High-resolution HAADF STEM general view of the carbon support, Pt and the Ta-oxide network; (b) detailed view of the Pt and Ta-oxide network showing the single Ta atoms of the oxide network (the oxygen atoms are not visible in this imaging condition); (c) overview of intricate Ta-Ox network on carbon support and strong interaction between the Pt catalysts only located on (or surrounded by) the Ta-oxide.

properties. In other words, behaving as the unique, even ideal electrocatalytic system for substantiation of the revertible cell assembly for spontaneous reversible alterpolar interchanges between PEMFC and WE, though still being based on unavoidable Pt catalysts. Meanwhile, since nanostructured Pt clusters are grafted and interbonding fixed upon hypo-d-oxide support, just confirmed by UHRTEM nanoimages, their lifetime has been dramatically increased (at least doubled), there is no agglomeration, nor hydrogen crossover through PEM, and there is now provided ability for prevailing Pt recovery. Namely, the substance consists in the reversible alterpolar interchangeable electrocatalytic operation with pronounced spillover (both Pt−H and Pt−OH) abilities; then the bifunctional (PEMFC versus WE) cell construction is a simple routine engineering task.

CONCLUSIVE REMARKS

Authors dealing with nanostructured electrocatalysts for L&MT PEMFCs usually use to infer that nanostructured Pt (Pt/C) among individual metals best satisfies all catalytic requirements. Such statement entirely concerns the HER, but by no means relates to the ORR and OER (Figure 1a,b). In other words, there usually imposes a rather broad polarization range (Figure 1b) between the preceding primary and surface oxides reactive interchanging and interfering potential interval, or simple adsorption/desorption within the reversible Pt−OH peaks, separating the latter by the pronouncedly high energy barrier from oxygen evolving limits (and/or the initial ORR range in the reverse scan direction) in both potentiodynamic sweep directions, and this way making platinum dramatically less noble and nonresponding for the overall electrocatalytic requirements. Meanwhile, the present paper deals with and has pointed out that the properly selected interactive (SMSI) hypo-d-d- and in particular some hypo-d-f- mixed valence oxide supports in many composite combinations, initially and continuously (enough water vapor feeding supply!) provide the enriched latent storage of the primary oxides within the critical potential interval and thence fill the gap in both anodic and cathodic scan directions, and all along the potential axis between hydrogen and oxygen evolving limits, similarly as within the standard classical reversible peak position for the Pt−OH generation and the energy source of the latter (Figure 1a). Such interactive induced support occurrences are indispensable and unavoidably necessary for the interfering spillover and corresponding interference between Pt−OH and Pt═O, enabling the enhanced electrocatalytic reaction to proceed (eq 3c), and finally making Pt reversible and more electrocatalytically 'noble' for the ORR. This is the core achievement and main contribution of the present study. In fact, several (and even many) mixed valence hypo-d-oxide compounds, in particular when properly doped by hypo-f-oxides, impose the reversible properties all along the potential axis between hydrogen and oxygen evolving limits in aqueous media, but not exactly for very high current density loads (preferably at

dx.doi.org/10.1021/jp412292w | J. Phys. Chem. C XXXX, XXX, XXX−XXX

about 1.0 A·cm^{-2}), and require further optimization. However, one has to distinguish between the reversible and the ideally (theoretical definition only) reversible electrode features. The optimization primarily concerns the doping effect of Gd (the highest elemental paramagnetic susceptibility available), Ho, La, Y, even Mo, Hf, Zr, so far never tried. Meanwhile, the striking point has been that the higher the specific amount of interactive supporting (SMSI) mixed valence hypo-d- and/or hypo-d-f-oxides per surface unit of exposed Pt (or Au, etc.) catalyst, within their rather high amounts and ratios, the higher the latent storage of corresponding primary oxides (Figures 6, 7, and 8), the more pronounced their spillover spreading rate becomes, and thence the more facilitated becomes their interfering catalytic reaction with the surface oxide (eq 3c), and consequently, the more pronounced the overall ORR rate and the whole electrocatalytic effect and yields. In other words, the primary oxide spillover growth increases and consequently, in the same proportion, increases the overall electrocatalytic rate and effect for the ORR.

It has also been pointed out that while the reversible potential range along the Tafel plots is associated with the adsorptive (Pt−OH/Pt═O) oxide deposits, the highly polarizable features are the property of clean, oxide deprived plain metallic Pt surface. Consequently, the entire electrocatalytic activation consists in the extension of the former all along the potential axis between the hydrogen and oxygen evolving limits, by the extra stable interactive deposited and strong d-d-bonding hypo-d-f-oxide mixed valence composites upon nanostructured Pt for the primary oxide generating and enabling its pronounced latent storage; fortunately, the majority of them feature extra high stability both in mineral acid and alkaline aqueous media, many even possess very high electron conductivity (over 300 S·cm^{-1}), thereby enabling even complete replacement of carbon nanostructured current collection particles.

The embodiment and substantiation of such composite electrocatalysts with the ROE features, mostly for the ORR, then primarily consists in the strong hypo-hyper-d-d- (or, -d-f-) interactive bonding (exampled nanostructured Pt/Nb_2O_5,TiO_2,-CeO_2/C, or Pt/Ta_2O_5,TiO_2,LaO_2/C), that behaves as the same body, and thereby keeps almost endlessly its electrocatalytic activity. The solid hypo-d-f-oxide part then establishes the strong bonding effectiveness with Pt (or Au) and keeps the high electronic conductivity ties, while its hydrated surface undertakes the latent storage and continuous Pt−OH spillover supply of the catalytic metal. So far rough estimations point to the doubled Pt lifetime in LT PEMFCs, when strongly interactive and selective grafting bonded upon mixed valence hypo-d-f-oxide supports, that is of substantial importance and still can be further advanced.

In short, the interfering core features tuned in interactive harmony for embodiment and operating of such advanced electrocatalysts with the ROE properties have been: (i) The strong (SMSI) hyper-hypo-d-d-interelectronic bonding and embodiment of one-body catalytic metal−support composite nanostructure: Pt/Nb_2O_5,TiO_2. (ii) Spontaneous dissociative adsorption of water molecules upon hypo-d-oxide surface (Pt/TiO_2/$Ti(OH)_4$), enabling hydroxide ions membrane transfer, ending up with Pt−OH spillover under electrode polarization. (iii) Providing electronic conductivity of nonhydrated interbonded composite hypo-d-oxides in between (Pt/Nb_2O_5,TiO_2/$Ti(OH)_4$,$Nb(OH)_5$, the external hydrated part featuring the high latent storage of Pt−OH, under polarization immediately starts its spillover. The similar procedure occurs with the same bronze type nanostructured composite electrocatalyst, but now based on H-adatoms spillover. As the overall sublimation, it has been substantiated that the reversible alterpolar bronze-type electrocatalysts enable advanced revertible cell altering between PENFCs and WE.

AUTHOR INFORMATION

Corresponding Author

*E-mail: jelena@iceht.forth.gr; phone: +30-2610-435754.

Notes

The authors declare no competing financial interest.

Biographies

Professor Milan M. Jaksic graduated with a degree in physical chemistry from the Faculty of Technology and Metallurgy (TMF), University of Belgrade (1958, grade 9.1/10), and immediately became the Manager of Chlorine and Chlorate Plants (1958−1966), Factory 'Jugovinil', near Split, Croatia, where he started his doctorate thesis and was chosen for the Lecturer in Electrochemical Processes of the Faculty of Technology, University of Split (1963). He was the principal investigator and founder of the Laboratory of Industrial Electrochemistry at Center of Electrochemistry, IHTM, Belgrade (1966-78). HE obtained his Ph.D. degree at TMF-UB in Advances in Electrochemical Chlorate Cell Process, with Professor A.R. Despic as his supervisor, in 1970. He was also a Fulbright−Huys grantee for postdoc studies in Electrochemical Engineering (Hydrodynamic Effects on Macromorphology of Zinc Electrodeposits and Flow Visualisation) with Professor C.W. Tobias, in the Department of Chemical Engineering and LBL, University of California, Berkeley, 1976−78. Hs was a professor in Physical Chemistry at the Institute of Food Technology, Faculty of Agriculture, University of Belgrade (1978 −2000). He also held the following visiting professorships: (i) University of California, Berkeley with Professor John Newman, 1984; (ii) Laboratory of Industrial Electrochemistry, NTNU, University of Trondheim, Norway, with Professor R. Tunold, 1989/90; Department of Chemical Engineering, and ICEHT/FORTH, University of Patras, Greece with Professor C.G. Vayenas, 1992/94, 2000/01, and on strategic EU projects in PEMFC Electrocatalysis with Dr. S.G. Neophytides, 2001/04, Honored International Affiliated Member at ICEHT/FORTH, 2010 -, www.iceht.forth.gr. Awards: (i) Prestigious October Belgrade city Award, 1974; (ii) 'Sir William Grove Award', IAHE (International Association for Hydrogen Energy), for "outstanding contributions to the theory of electrocatalysis for hydrogen electrode reactions", 2006, and (iii) Annual award of Union of University Professors of Serbia, 1999. He has published more than 120 peer reviewed scientific papers mostly in electrocatalysis for oxygen and hydrogen electrode reactions, SCI about 3,000.

dx.doi.org/10.1021/jp412292w | J. Phys. Chem. C XXXX, XXX, XXX−XXX

Professor Gianluigi Botton received a degree in Engineering Physics and a Ph.D. in Materials Engineering at Ecole Polytechnique of Montreal. He was a Postdoctoral Fellow in the Department of Materials Science and Metallurgy at the University of Cambridge from 1993 to 1998. He joined the Materials Technology Laboratory of Natural Resources Canada (NRCan) in 1998 as a research scientist. In 2001 he moved to the Department of Materials Science and Engineering at McMaster University where he was awarded a Tier 1 Canada Research Chair in Electron Microscopy of Nanoscale Materials. He received the Brian Ives Lectureship of the ASM in 2009 and the CAMBR Lectureship at Western University in 2013 and the NABMM Scientific Merit Award at NRCan. He established, and currently leads, the Canadian Centre for Electron Microscopy a national facility for ultrahigh-resolution microscopy. His area of expertise is Analytical Electron Microscopy-AEM of nanostructured materials. He is regularly invited to present lectures on the application of microscopy and energy loss spectroscopy (EELS) in catalysts and plasmonics. He wrote five book chapters on microscopy techniques, including the reference on AEM in the Encyclopedia *Science of Microscopy* (Springer) and on EELS in the book *STEM* (Springer). He was a past president of the Microscopical Society of Canada and he is the Editor of *Microscopy*, and on the editorial board of *Micron*, two international journals dedicated the development and application of microscopy methods.

Dr. Georgios Papakonstantinou received his diploma in Chemical Engineering from the National Technical University of Athens in 2001. He completed his Ph.D. in Chemical Engineering at the University of Patras in 2010 under the supervision of Prof. C.G. Vayenas, Member of Greek National Academy of Sciences and Arts, Athens, and Dr. S. G. Neophytides studying the CO tolerance of bimetallic and ternary electrocatalysts in Polymer Electrolyte Fuel Cells, and continued working in the same area at the Institute of Chemical Engineering Science and High Temperature Chemical Processes/Foundation of Research and Technology, Hellas (ICEHT/FORTH) in Patras as a postdoc (2010–2011). Presently he is a research fellow at Joint Research Centre–Institute for Energy and Transport (JRC-IET) in Petten, Netherlands. His research has expanded to studying electrode processes in medium temperature polymer electrolyte fuel cells, as well as the degradation phenomena.

Feihong Nan received a BEng (2006) and MAsc (2008) in Materials Science and Engineering, respectively from Kunming University Science & Technology and McMaster University. She is currently enrolled in the Ph.D. program at McMaster University. She has developed expertise in electron microscopy and in particular scanning transmission electron microscopy and electron tomography.

Dr. Jelena M. Jakšić graduated from the Faculty of Physical Chemistry, Faculties of Sciences, University of Belgrade, 1995, with two academic years of studies in the Departments of Physics and Chemical Engineering, University of Patras in Greece. Her diploma thesis with Professor S. Mentus on *Non-Faradaic Electrochemical Modification of Catalytic Activity (NEMCA) for Heterogeneous* Reaction *of Hydrogen Oxidation in Aqueous Media* was awarded the Belgrade October city prize for creative contributions of youth, 1997. She obtained her M.S. at the Center for Multidisciplinary Studies, University of Belgrade, Surface State division, 2000, with Professors N. Krstajić, M. Vojnović, and N. Ristić on *Kinetics of Hydrogen Evolution on Intermetallic Phases and Alloys of Ni, Co and Mo*. She obtained her Ph.D. degree at Faculty of Technology and Metallurgy, Univerrsity of Belgrade, 2004, with partial fulfillment at Department of Chemical Engineering, University of Patras, Greece, within two EU research projects, "Prometheas" and "Apollon", on *Kinetics of Electrochemical Hydrogen Evolution and Oxidation Reactions on Mo–Pt Alloys* carried out with Professor N. Krstajic; she also received a one-year Greek Ministry of Science grant for Ph.D. thesis work with Dr. S. G. Neophytides. She has published 19 peer reviewed scientific papers; SCI about 350.

dx.doi.org/10.1021/jp412292w | *J. Phys. Chem. C* XXXX, XXX, XXX–XXX

■ ACKNOWLEDGMENTS

Experiments in the present paper have been carried out at the Institute of Chemical Engineering Sciences (ICEHT), FORTH, Patras, Greece, and the Department of Materials Science & Engineering, McMaster University, Hamilton, Ontario, L8S 4M1, Canada.

■ REFERENCES

(1) *Handbook of Fuel Cells. Fundamentals, Technology and Applications*; Vielstich, W.; Lamm, A.; Gasteiger, H. A.; Eds.; Wiley: Chichester, England, 2003; Vols. *1*−*4*.

(2) Conway, B. E. Electrochemical Oxide Film Formation at Noble Metals as a Surface-Chemical Process. *Prog. Surf. Sci.* **1995**, *49*, 331−452.

(3) Angerstein-Kozlowska, H.; Conway, B. E.; Sharp, W. B. A. The Real Condition of Electrochemically Oxidized Platinum Surfaces: Part I. Resolution of Component Processes. *J. Electroanal. Chem.* **1973**, *43*, 9−36.

(4) Angerstein-Kozlovska, H.; Conway, B. E.; Hamelin, A.; Stoicoviciu, L. Elementary Steps of Electrochemical Oxidation of Single-Crystal Planes of Au. I. Chemical Basis of Processes Involving Geometry of Anions and the Electrode Surfaces. *Electrochim. Acta* **1986**, *31*, 1051−1061.

(5) Angerstein-Kozlowska, H.; Conway, B. E.; Hamelin, A.; Stoicoviciu, L. Elementary Steps of Electrochemical Oxidation of Single-Crystal Planes of Au. II. A Chemical and Structural Basis of Oxidation of the (111) Plane. *J. Electroanal. Chem.* **1987**, *228*, 429−453.

(6) Hoare, J. P. On the Interaction of Oxygen with Platinum. *Electrochim. Acta* **1982**, *27*, 1751−1761.

(7) Ma, Y.; Balbuena, P. B. Designing Oxygen Reduction Catalysts: Insights from Metalloenzymes. *Chem. Phys. Lett.* **2007**, *440*, 130−133.

(8) Neophytides, S. G.; Zafeiratos, S.; Jaksic, M. M. Selective Interactive Grafting of Composite Bifunctional Electrocatalysts for Simultaneous Anodic Hydrogen and CO Oxidation, I. Theoretical Concepts and Embodiment of Novel Type Composite Catalysts. *J. Electrochem. Soc.* **2003**, *150*, E512−E526.

(9) Neophytides, S. G.; Murase, K.; Zafeiratos, S.; Papakonstantinou, G.; Paloukis, F. E.; Krstajic, N. V.; Jaksic, M. M. Composite Hypo-Hyper-d-Intermetallic Phases as Supported Interactive Electrocatalysts. *J. Phys. Chem. B* **2006**, *110*, 3030−3042.

(10) Jaksic, J. M.; Krstajic, N. V.; Vracar, Lj. M.; Neophytides, S. G.; Labou, D.; Falaras, P.; Jaksic, M. M. Spillover of Primary Oxides as a Dynamic Catalytic Effect of Interactive Hypo-d-Oxide Supports. *Electrochim. Acta* **2007**, *53*, 349−361.

(11) Krstajic, N. V.; Vracar, Lj. M.; Radmilovic, V. R.; Neophytides, S. G.; Labou, D.; Jaksic, J. M.; Tunold, R.; Falaras, P.; Jaksic, M. M. Advances in Interactive Supported Electrocatalysts for Hydrogen and Oxygen Electrode Reactions. *Surf. Sci.* **2007**, *601*, 1949−1966.

(12) Zafeiratos, S.; Papakonstantinou, G.; Jaksic, M. M.; Neophytides, S. G. The Effect of Mo Oxides and TiO_2 Support on the Chemisorption Features of Linearly Adsorbed CO on Pt Crystallites: An Infrared and Photoelectron Spectroscopy Study. *J. Catal.* **2005**, *232*, 127−136.

(13) Jaksic, J. M.; Labou, D.; Papakonstantinou, G. D.; Siokou, A.; Jaksic, M. M. Novel Spillover Interrelating Reversible Electrocatalysts for Oxygen and Hydrogen Electrode Reactions. *J. Phys. Chem. C* **2010**, *114*, 18298−18312.

(14) Neophytides, S. G.; Zafeiratos, S.; Papkonstantinou, G. D.; Jaksic, J. M.; Paloukis, F. E.; Jaksic, M. M. Extended Brewer Hypo-Hyper-d-Interionic Bonding Theory, I. Theoretical Considerations and Examples for Its Experimental Confirmation. *Int. J. Hydrogen Energy* **2005**, *30*, 131−147.

(15) Neophytides, S. G.; Zafeiratos, S.; Papkonstantinou, G. D.; Jaksic, J. M.; Paloukis, F. E.; Jaksic, M. M. Extended Brewer Hypo-Hyper-d-Interionic Bonding Theory, II. Strong Metal-Support Interaction Grafting of Composite Electrocatalysts. *Int. J. Hydrogen Energy* **2005**, *30*, 393−410.

(16) Papakonstantinou, G. D.; Jaksic, J. M.; Labou, D.; Siokou, A.; Jaksic, M. M. Spillover Phenomena and Its Striking Impacts in Electrocatalysis for Hydrogen and Oxygen Electrode Reactions. *Adv. Phys. Chem.* **2011**, *2011*, 1−22 (Article ID 412165). http://www.hindawi.com/journals/apc/psi/.

(17) Volkening, S.; Bedurftig, K.; Jacobi, K.; Wintterlin, J.; Ertl, G. Dual Path Mechanism for Catalytic Oxidation of Hydrogen on Platinum Surface. *Phys. Rev. Lett.* **1999**, *83*, 2672−2675.

(18) Bockris, J. O'M.; Shamshul Huq, A. K. M. The Mechanism of the Electrolytic Evolution of Oxygen on Platinum. *Proc. Royal Soc. (London). Ser. A, Math. Phys, Sci, (1934−1990)* **1956**, *237*, 277−296.

(19) Masud, J.; Alam, M. T.; Okajima, T.; Ohsaka, T. The Mechanism of the Electrolytic Evolution of Oxygen on Platinum. *Chem. Lett. Japan* **2011**, *40*, 252−254.

(20) Masud, J.; Alam, M. T.; Miah, M. R.; Okajima, T.; Ohsaka, T. Enhanced Electrooxidation of Formic Acid at Ta_2O_5-Modified Pt Electrode. *Electrochem. Commun.* **2011**, *13*, 86−89.

(21) Awaludin, Z.; Suzuki, M.; Masud, J.; Okajima, T.; Ohsaka, T. Enhanced Electrocatalysis of Oxygen Reduction on Pt/TaO_x/GC. *J. Phys. Chem. C* **2011**, *115*, 25557−25567.

(22) Awaludin, Z.; Moo, J. G. S.; Okajima, T.; Ohsaka, T. TaO_x-Capped Pt Nanoparticles as Active and Durable Electrocatalysts for Oxygen Reduction. *J. Mater. Chem, A* **2013**, *1*, 14754−14765.

(23) Ferdousi, B. N.; Islam, M. M.; Okajima, T.; Mao, L.; Ohsaka, T. Enhanced Catalytic Reduction of Oxygen at Tantalum Deposited Platinum Electrode. *Chem. Commun.* **2010**, *46*, 1165−1167.

(24) Masuda, T.; Fukumitsu, H.; Fugane, K.; Togasaki, H.; Matsumura, D.; Tamura, K.; Nishihata, Y.; Yoshikawa, H.; Kobayashi, K.; Mori, T.; et al. Role of Cerium Oxide in the Enhancement of Activity for the Oxygen Reduction Reaction at Pt-CeO_x Nanocomposite Electrocatalyst − An in Situ Electrochemical X-ray Absorption Fine Structure Study. *J. Phys. Chem. C* **2012**, *116*, 10098−10102.

(25) Fugane, K.; Mori, T.; Ou, D. R.; Suzuki, A.; Yoshikawa, H.; Masuda, T.; Uosaki, K.; Yamashita, Y.; Ueda, S.; Kobayashi, K.; et al. On Small Amount of Amorphous CeO_x Promoted Pt Cathode for Fuel Cell Application. *Electrochim. Acta* **2011**, *56*, 3874−3883.

(26) Ou, D. R.; Mori, T.; Togasaki, H.; Takahashi, M.; Ye, F.; Drennan, J. Microstructural and Metal-Support Interactions of the Pt-CeO_2/C Catalysts for Direct Methanol Fuel Cell Application. *Langmuir* **2011**, *27*, 3859−3866.

(27) Fugane, K.; Mori, T.; Ou, D. K.; Yan, P.; Ye, F.; Yoshikawa, H.; Drennan, J. Improvement of Cathode Performance on Pt−CeO_x by Optimization of Electrochemical Pretreatment Condition for PEMFC Application. *Langmuir* **2012**, *28*, 16692−16700.

(28) Ou, D. R.; Mori, T.; Fugane, K.; Togasaki, H.; Ye, F.; Drennan, J. Stability of Ceria Supports in Pt−CeO_x/C Catalysts. *J. Phys. Chem. C* **2011**, *115*, 19239−19245.

(29) Koper, M. T. M.; Van Santen, R. A. Interaction of H, O and OH with Metal Surfaces. *J. Electroanal. Chem.* **1999**, *472*, 126−136.

(30) Tseung, A. C. C.; Shen, P. K.; Chen, K. Y. Precious Metal/Hydrogen Bronze Anode Catalysts for the Oxidation of Small Organic Molecules and Impure Hydrogen. *J. Power Sources* **1996**, *61*, 223−225.

(31) Tseung, A. C. C.; Chen, K.-Y. Hydrogen Spillover Effect on Pt/WO_3 Anode Catalyst. *Catal. Today* **1997**, *38*, 439−443.

(32) Shen, P. K.; Chen, K.-Y.; Tseung, A. C. C. Performance of Co-electrodeposited Pt−Ru/WO_3 Electrodes for the Electrooxidation of Formic Acid at Room Temperature. *J. Electroanal. Chem.* **1995**, *389*, 223−225.

(33) Glemser, O.; Naumann, K. Kristallisierte Wolframblauverbindungen; Wasserstoffanaloga der Wolframbronzen H_xWO_3. *Z. Anorg. Allg. Chem.* **1951**, *265*, 288−302.

(34) Sasaki, K.; Zhang, L.; Adzic, R. R. Niobium Oxide-Supported Platinum Ultra-Low Amount Electrocatalysts for Oxygen Reduction. *Phys. Chem. Chem. Phys.* **2008**, *10*, 159−167.

(35) Fuentes, R. E.; Garcia, B. L.; Weidner, J. W. A Nb-Doped TiO_2 Electrocatalyst for Use in Direct Methanol Fuel Cells. *ECS Trans.* **2008**, *12*, 239−248.

(36) Elezović, N. R.; Babić, B. M.; Gajić-Krstajić, Lj.; Radmilović, V.; Krstajić, N. V.; Vračar, Lj. Synthesis, Characterization and Electrocatalytic Behavior of Nb−TiO_2/Pt Nanocatalyst for Oxygen Reduction Reaction. *J. Power Sources* **2010**, *195*, 3961−3968.

(37) Elezovic, N. R.; Babic, B. M.; Radmilovic, V. R.; Vracar, Lj. M.; Krstajic, N. V. Nb−TiO_2 Supported Platinum Nanocatalyst for Oxygen Reduction Reaction in Alkaline Solutions. *Electrochim. Acta* **2011**, *56*, 9020−9026.
(38) Chen, G.; Bare, S. R.; Mallouk, T. E. Development of Supported Bifunctional Electrocatalysts for Unitized Regenerative Fuel Cells. *J. Electrochem. Soc.* **2002**, *149*, A1092−A1099.
(39) Micoud, F.; Maillard, F.; Gourgaud, A.; Chatenet, M. Unique CO-Tolerance on Pt−WO_x Materials. *Electrochem. Commun.* **2009**, *11*, 651−654.
(40) Park, K. W.; Seul, K. S. Nb−TiO_2 Supported Pt Cathode Catalyst for Polymer Electrolyte Membrane Fuel Cells. *Electrochem. Commun.* **2007**, *9*, 2256−2260.
(41) Huang, S.-Y.; Ganesan, P.; Popov, B. N. Electrocatalytic Activity and Stability of Niobium-Doped Titanium Oxide Supported Platinum Catalyst for Polymer Electrolyte Membrane Fuel Cells. *Appl. Catal., B* **2010**, *96*, 224−231.
(42) Chhina, H.; Campbell, S.; Kesler, O. *Ex Situ* and *In Situ* Stability of Platinum Supported on Niobium-Doped Titania for PEMFCs. *J. Electrochem. Soc.* **2009**, *156*, B1232−B1237.
(43) Zhang, L.; Wang, L.; Holt, C. M. B.; Navessin, T.; Malek, K.; Eikerling, M. H.; Mitlin, D. Oxygen Reduction Reaction Activity and Electrochemical Stability of Thin-Film Bilayer Systems of Platinum on Niobium Oxide. *J. Phys. Chem. C* **2010**, *114*, 16463−16474.
(44) Lee, K.-S.; Yoo, S. J.; Nah, Y.-C.; Kim, H. S.; Park, K.-S.; Yun, J. W. Oxygen Reduction Reaction of Pt Supported on Y-doped $SrTiO_3$. *Electrochem. Solid-State Lett.* **2012**, *15*, B61−B64.
(45) Nishanth, K. G.; Sridhar, P.; Pitchumani, S. Enhanced Oxygen Reduction Reaction Activity Through Spillover Effect by Pt−$Y(OH)_3$/C Catalyst in Direct Methanol Fuel Cells. *Electrochem. Commun.* **2011**, *13*, 1465−1468.
(46) Bokhimi, X.; Morales, A.; Novaro, O.; Lopez, T.; Sanchez, E.; Gomez, R. Effect of Hydrolysis Catalyst on the Ti Deficiency and Crystallite Size of Sol-Gel-TiO_2 Crystalline Phases. *J. Mater. Res.* **1995**, *10*, 2788−2796.
(47) Chaparro, A. M. Study of Spillover Effects with the Rotating Disk Electrode. *Electrochim. Acta* **2011**, *58*, 691−698.
(48) Kou, R.; Shao, Y.; Mei, Z.; Nie, Z.; Wang, D.; Wang, C.; Viswanathan, V. V.; Park, S.; Aksay, I. A.; Lin, Y.; et al. Stabilization of Electrocatalytic Metal Nanoparticles at Metal-Metal Oxide-Graphen Triple Junction Points. *J. Am. Chem. Soc.* **2011**, *133*, 2541−2547.
(49) Teichner, S. J. Recent Studies in Hydrogen and Oxygen Spillover and Their Impact on Catalysis. *Appl. Catal.* **1990**, *62*, 1−10.
(50) Furukawa, S.; Shishido, T.; Teramura, K.; Tanaka, T. Photocatalytic Oxidation of Alcohols Over TiO_2 Covered with Nb_2O_5. *ACS Catal.* **2012**, *2*, 175−179.
(51) Michalow, K. A.; Flak, A.; Heel, A.; Parlinska-Wojtan, M.; Rekas, M.; Graule, T. Effect of Nb Doping on Structural, Optical and Photocatalytic Properties of Flame-Made TiO_2 Nanopowder. *Environ. Sci. Pollut. Res.* **2012**, *19*, 3696−3708.
(52) Hirano, M.; Ito, T. Effect of Co-dopant on the Formation and Properties of Anatase-Type Titania Solid Solutions Doped with Niobium. *J. Phys. Chem. Solids* **2011**, *72*, 661−666.
(53) Kubacka, A.; Colón, G.; Fernández-García, M. Cationic (V, Mo, Nb, W) Doping of TiO_2−Anatase: A Real Alternative for Visible Light-Driven Photocatalysts. *Catal. Today* **2009**, *143*, 286−292.
(54) Hirano, M.; Matsushima, K. Effect of Niobium on the Structure and Photoactivity of Anatase (TiO_2) Nanoparticles. *J. Nanosci. Nanotechnol.* **2006**, *6*, 762−770.
(55) Kudo, A.; Kato, H.; Nakagawa, S. Water Splitting Into H_2 and O_2 on New $Sr_2M_2O_7$ (M = Nb and Ta) Photocatalysts with Layered Perovskite Structures, Factors Affecting the Photocatalytic Activity. *J. Phys. Chem. B* **2000**, *104*, 571−575.
(56) Ristic, N. M.; Kotorcevic, M.; Lacnjevac, C. M.; Jokic, A. M.; Jaksic, M. M. Some Specific Potentiodynamic Behavior of Certain Aldehydes and Monosaccharides. 1. Some Simple and Some Specific Aldehydes. *Electrochim. Acta* **2000**, *45*, 2973−2989.
(57) Zhang, X.; Chan, K.-Y.; Tseung, A. C. C. Electrochemical Oxidation of Glucose by Pt/WO_3 Electrode. *J. Electroanal. Chem.* **1995**, *386*, 241−243.
(58) Guldberg, C. M.; Waage, P. Ueber die chemische Affinität. § 1. Einleitung. *J. Prakt. Chem.* **1879**, *19*, 69−114. Lund, E. W. *J. Chem. Educ.* **1965**, *42*, 548−550.
(59) Vittadini, A.; Selloni, A.; Rotzinger, F. P.; Gratzel, M. Structure and Energetics of Water Adsorbed at TiO_2 Anatase (101) and (001) Surfaces. *Phys. Rev. Lett.* **1998**, *81*, 2954−2957.
(60) Lazzeri, M.; Vittadini, A.; Selloni, A. Structure and Energetics of Stoichiometric TiO_2 Anatase Surfaces. *Phys. Rev. B* **2001**, *63*, No. 155409.
(61) Tilocca, A.; Selloni, A. Reaction Pathway and Free Energy Barrier for Defect-Induced Water Dissociation on the (101) Surface of TiO_2−Anatase. *J. Chem. Phys.* **2003**, *119*, 7445−7451.
(62) Boudart, M.; Vannice, M. A.; Benson, J. E. Adlineation, Portholes and Spillover. *Z. Phys. Chem., N.F.* **1969**, *64*, 171−177.
(63) Kohn, H. W.; Boudart, M. Reaction of Hydrogen with Oxygen Adsorbed on a Platinum Catalyst. *Science* **1964**, *145*, 149−150.
(64) Benson, J. E.; Kohn, H. W.; Boudart, M. On the Reduction of Tungsten Trioxide Accelerated by Platinum and Water. *J. Catal.* **1966**, *5*, 307−313.
(65) Vannice, M. A.; Boudart, M.; Fripiat, J. J. Mobility of Hydrogen in Hydrogen Tungsten Bronze. *J. Catal.* **1970**, *17*, 359−365.
(66) Livage, J.; Henry, M.; Sanchez, C. Sol−Gel Chemistry of Transition Metal Oxides. *Prog. Solid State Chem.* **1988**, *18*, 259−341.
(67) Judeinstein, P.; Livage, J. Sol−Gel Synthesis of WO_3 Thin Films. *J. Mater. Chem.* **1991**, *1*, 621−627.
(68) Livage, J.; Guzman, G. Aqueous Precursors for Electrochromic Tungsten Oxide Hydrates. *Solid State Ionics* **1996**, *84*, 205−211.
(69) Tauster, S. J.; Fung, S. C.; Baker, R. T. K.; Horsley, J. A. Strong-Interactions in Supported-Metal Catalysts. *Science* **1981**, *211*, 1121−1125.
(70) Tauster, S. J.; Fung, S. C. Strong Metal-Support Interactions: Occurrence Among the Binary Oxides of Groups IIA−VB. *J. Catal.* **1978**, *55*, 29−35.
(71) Stevenson, S. A., *Metal-Support Interaction in Catalysis, Sintering and Redispersion*; Van Nostrand: New York, 1987.
(72) Haller, G. L.; Resasco, D. E. Metal−Support Interaction: Group VIII Metals and Reducible Oxides. In *Advances in Catalysis*; Eley, D. D., Pires, H., Weisz, P. B., Eds.; Academic Press: San Diego, 1989; *Vol. 36*, pp 173−235.
(73) Brewer, L. Bonding and Structures of Transition Metals. *Science* **1968**, *161*, 115−122.
(74) Jaksic, M. M. Hypo-Hyper-d-Electronic Interactive Nature of Synergism in Catalysis and Electrocatalysis for Hydrogen Reactions. *Electrochim. Acta* **2000**, *45*, 4085−4099.
(75) Lueking, A. D.; Yang, R. T. Hydrogen Spillover to Enhance Hydrogen Storage − Study of the Effect of Carbon Physicochemical Properties. *Appl. Catal. A: General* **2004**, *265*, 259−268.
(76) Kim, J.-G.; Regalbuto, J. R. The Effect of Calcination on H_2 Spillover in Pt/MoO_3, II. Kinetics. *J. Catal.* **1993**, *139*, 175−190.
(77) Agarwal, R. K.; Noh, J. S.; Schwarz, J. A. Effect of Surface Acidity of Activated Carbon on Hydrogen Storage. *Carbon* **1987**, *25*, 219−226.
(78) Takagi, H.; Hatori, H.; Yamada, Y. Reversible Adsorption/Desorption Property of Hydrogen on Carbon Surface. *Carbon* **2005**, *43*, 3037−3039.
(79) Mavrikakis, M.; Stoltze, P.; Norskov, J. K. Making Gold Less Noble. *Catal. Lett.* **2000**, *64*, 101−106.
(80) Schmidt, T. J.; Gasteiger, H. A.; Stab, G. D.; Urban, P. M.; Kolb, D. M.; Behm, R. J. Characterization of High-Surface-Area Electrocatalysts Using a Rotating Disk Electrode Configuration. *J. Electrochem. Soc.* **1998**, *145*, 2354−2358.
(81) Boskovic, I.; Mentus, S. V.; Pjescic, J. M. Ta_2O_5 Templated Growth of Droplet-Like Platinum Particles by Potentiodynamic Polarization of Tantalum in Aqueous Solution of Hexachloroplatinic Acid. *Electrochem. Commun.* **2005**, *7*, 797−802.

(82) Savadogo, O. Surface Chemistry and Electrocatalytic Activity of the HER on Nickel Modified with Heteropolyacids. *J. Electrochem. Soc.* **1992**, *139*, 1082−1087.
(83) Hadzi-Jordanov, S.; Angerstein-Kozlowska, H. A.; Vukovic, M.; Conway, B. E. Reversibility and Growth Behavior of Surface Oxide Films at Ruthenium Electrode. *J. Electrochem. Soc.* **1978**, *125*, 1471−1480.
(84) Riess, I.; Vayenas, C. G. Fermi Level and Potential Distribution in Solid Electrolyte Cells with and without Ion Spillover. *Solid State Ionics* **2003**, *159*, 313−329.
(85) Trasatti, S. The Work Function in Electrochemistry. In *Advances in Electrochemistry and Electrochemical Engineering*; Tobias, C. W., Goerischer, H., Eds.; Interscience: New York, 1977; Vol. *10*, pp 213−321.
(86) Vayenas, C. G.; Bebelis, S.; Pliangos, C.; Brosda, S.; Tsiplakides, D. *Electrochemical Activation of Catalysis: Promotion, Electrochemical Promotion, and Metal−Support Interactions*; KluverAcademic/Plenum Publishers: New York, 2001.
(87) Vayenas, C. G.; Jaksic, M. M.; Bebelis, S. I.; Neophytides, S. G. The Electrochemical Activation of Catalytic Reactions. In *Modern Aspects of Electrochemistry*; Bockris, J. O'M., Conway, B. E., White, R. E., Eds.; Plenum Press: New York, 1996; Vol. *29*, pp 57−202.
(88) Vayenas, C. G.; Bebelis, S.; Ladas, L. The Dependence of Catalytic Activity on Catalyst Work Function. *Nature* **1990**, *343*, 625−627.
(89) Tsiplakides, D.; Nicole, J.; Vayenas, C. G.; Comninellis, Ch. Work Function and Catalytic Activity Measurements of an IrO_2 Film Deposited on YSZ Subjected to *In Situ* Electrochemical Promotion. *J. Electrochem. Soc.* **1998**, *145*, 905−908.
(90) Neophytides, S.; Tsiplakides, D.; Stonehart, P.; Jaksic, M. M.; Vayenas, C. Electrochemical Enhancement of a Catalytic Reaction in Aqueous Solution. *Nature* **1994**, *370*, 45−47.
(91) Neophytides, S. G.; Tsiplakides, D.; Stonehart, P.; Jaksic, M. M.; Vayenas, C. G. Non-Faradaic Electrochemical Modification of the Catalytic Activity of Pt for H_2 Oxidation in Aqueous Alkaline Media. *J. Phys. Chem.* **1996**, *100*, 14803−14814.
(92) Tsiplakides, D.; Neophytides, S. G.; Enea, O.; Jaksic, M. M.; Vayenas, C. G. Non-Faradaic Electrochemical Modification of the Catalytic Activity of Pt-Black Electrodes Deposited on Nafion 117 Solid Polymer Electrodes. *J. Electrochem. Soc.* **1997**, *144*, 2072−2078.
(93) Tsiplakides, D.; Vayenas, C. G. Electrode Work Function and Absolute Potential Scale in Solid-State Electrochemistry. *J. Electrochem. Soc.* **2001**, *148*, E189−E202.
(94) Tsiplakides, D.; Archonta, D.; Vayenas, C. G. Absolute Potential Measurements in Solid and Aqueous Electrochemistry Using Two Kelvin Probes and Their Implications for the Electrochemical Promotion of Catalysts. *Topics Catal.* **2007**, *44*, 469−479.
(95) Trasatti, S. The Concept of Absolute Electrode Potential. An Attempt at a Calculation. *J. Electroanal. Chem.* **1982**, *139*, 1−13.
(96) Nicole, J.; Tsiplakides, D.; Pliangos, C.; Verykios, X. E.; Comninellis, Ch.; Vayenas, C. G. Electrochemical Promotion and Metal−Support Interactions. *J. Catal.* **2001**, *204*, 23−34.
(97) Metcalfe, I. S. Electrochemical Promotion of Catalysts, I. Thermodynamic Considerations. *J. Catal.* **2001**, *199*, 247−258.
(98) Metcalfe, I. S. Electrochemical Promotion of Catalysts, II. The Role of a Stable Spillover Species and Prediction of Reaction Rate Modification. *J. Catal.* **2001**, *199*, 259−272.
(99) Markovic, N. M.; Ross, P. N. Surface Science Studies of Model Fuel Cell Electrocatalysts. *Surf. Sci. Rep.* **2002**, *45*, 117−229.
(100) Jaksic, M. M. Advances in Electrocatalysis for Hydrogen Evolution in the Light of the Brewer−Engel Valence-Bond Theory. *J. Mol. Catal.* **1986**, *38*, 161−202.
(101) Friedel, J.; Sayers, C. M. On the Role of d-d-Electron Correlations in the Cohesion and Ferromagnetism of Transition Metals. *J. Phys. (Paris)* **1977**, *38*, 697−705.
(102) Gschneidner, K. A. Physical Properties and Interrelations of Metallic and Semimetallic Elements. In *Solid State Physics, Advances in Research and Applications*; Seitz, F., Turnbull, D., Eds.; Academic Press: New York, 1964; *Vol. 16*, pp 275−427.
(103) Jaksic, M. M. Volcano Plots along the Periodic Table, Their Causes and Consequences on Electrocatalysis for Hydrogen Electrode Reactions. *J. New Mater. Electrochem. Syst.* **2000**, *3*, 153−168.
(104) Methfessel, M.; Hennig, D.; Schefler, M. Trends of the Surface Relaxations, Surface Energies, and Work Functions of the 4d Transition Metals. *Phys. Rev. B* **1992**, *46*, 4816−4829.
(105) Jaksic, J. M.; Vracar, Lj. M.; Neophytides, S. G.; Zafeiratos, S.; Papakonstantinou, G. D.; Krstajic, N. V.; Jaksic, M. M. Structural Effects on Kinetic Properties for Hydrogen Electrode Reactions and CO Tolerance Along Mo−Pt Phase Diagram. *Surf. Sci.* **2005**, *598*, 156−173.
(106) Jaksic, M. M.; Lacnjevac, C. M.; Grgur, B. N.; Krstajic, N. V. Volcano Plots Along Intermetallic Hypo-Hyper-d-Electronic Phase Diagrams and Electrocatalysis for Hydrogen Electrode Reactions. *J. New Mater. Electrochem. Syst.* **2000**, *3*, 169−182.
(107) Jaksic, J. M.; Radmilovic, V. R.; Krstajic, N. V.; Lacnjevac, C. M.; Jaksic, M. M. Volcanic Periodicity Plots Along Transition Series, Hypo-Hyper-d-d-Interelectronic Correlations and Electrocatalysis for Hydrogen Electrode Reactions. *Macedonian J. Chem. Chem. Eng.* **2011**, *30*, 3−18.
(108) Peuckert, M.; Coenen, F. P.; Bonzel, H. P. XPS Study of the Electrochemical Surface Oxidation of Platinum in 1N H_2SO_4 Acid Electrolyte. *Electrochim. Acta* **1984**, *29*, 1305−1314.
(109) Drawdy, J. E.; Hoflund, G. B.; Gardner, S. D.; Yngvadottir, E.; Schryer, D. R. Effect of Pretreatment on a Platinized Tin Oxide Catalyst Used for Low-Temperature CO Oxidation. *Surf. Interface Anal.* **1990**, *16*, 369−374.
(110) Quaino, P.; Luque, N. B.; Nazmutdinov, R.; Santos, E.; Schmickler, W. Why is Gold Such a Good Catalyst for Oxygen Reduction in Alkaline Media? *Angew. Chem., Int. Ed.* **2012**, *51*, 1−5.
(111) Akita, T.; Tanaka, K.; Tsubota, S.; Haruta, M. Analytical High-Resolution TEM Study of Supported Gold Catalysts: Orientation Relationship Between Au Particles and TiO_2 Supports. *J. Electron Microsc.* **2000**, *49*, 657−662.
(112) Akita, T.; Lu, P.; Ichikawa, S.; Tanaka, K.; Haruta, M. Analytical TEM Study on the Dispersion of Au Nanoparticles in Au/TiO_2 Catalyst Prepared Under Various Temperatures. *Surf. Interface Anal.* **2001**, *31*, 73−78.
(113) Haruta, M. Size- and Support-Dependency in the Catalysis of Gold. *Catal. Today* **1997**, *36*, 153−166.
(114) Date, M.; Haruta, M. Moisture Effect on CO Oxidation Over Au/TiO_2 Catalyst. *J. Catal.* **2001**, *201*, 221−224.
(115) Boccuzzi, F.; Chiorino, A.; Tsubota, S.; Haruta, M. FTIR Study of Carbon Monoxide Oxidation and Scrambling at Room Temperature over Gold Supported on ZnO and TiO_2. *J. Phys. Chem.* **1996**, *100*, 3625−3631.
(116) Boccuzzi, F.; Chiorino, A.; Manzoli, M.; Lu, P.; Akita, T.; Ichikawa, S.; Haruta, M. Au/TiO_2 Nanosized Samples: A Catalytic, TEM, and FTIR Study of the Effect of Calcination Temperature on the CO Oxidation. *J. Catal.* **2001**, *202*, 256−267.
(117) Haruta, M. When Gold Is Not Noble: Catalysis by Nanoparticles. *Chem. Rec.* **2003**, *3*, 75−87.
(118) Hammer, B.; Norskov, J. K. Why Gold is the Noblest of All the Metals. *Nature* **1995**, *376*, 238−240.